Spring 5-3-2017

Insulin Nucleation Using Voltage Clamping and Current Clamping Techniques

Michael J. Bowen
mbowen13@student.gsu.edu

Insulin Nucleation Using Voltage Clamping and Current Clamping Techniques

by

MICHAEL BOWEN

Under the Direction of GANGLI WANG, PhD

ABSTRACT

Crystallization of proteins is the prerequisite to obtaining three-dimensional molecular structures; by X-ray crystallography. The knowledge of protein structures is foundational and could pave ways to the understanding of a protein's functions. However, obtaining single crystals is challenging and often a bottleneck let alone the need of satisfactory diffraction quality. In this thesis, quartz nanopipettes are used to spatially confine the location of nucleation and crystal growth at a nanometer scale. Current and voltage clamping techniques are employed to induce phase transition and subsequent crystal formation via external controls. Throughout the process, we can monitor and control the electrical current/potential that controls mass transport for local concentration adjustment.

INDEX WORDS: Crystallization, Insulin, Nucleation, Nanopipette, Current Clamping, Voltage Clamping, Transport at Nanoscale

Insulin Nucleation Using Voltage Clamping and Current Clamping Techniques

by

MICHAEL BOWEN

A Thesis Submitted in Partial Fulfillment of the Requirements for the Degree of

Masters of Science in Chemistry

in the College of Arts and Sciences

Georgia State University

2017

Insulin Nucleation Using Voltage Clamping and Current Clamping Techniques

by

MICHAEL BOWEN

Committee Chair: Dr. Gangli Wang

Committee: Gangli Wang

Ning Fang

Ming Luo

Electronic Version Approved:

Office of Graduate Studies

College of Arts and Sciences

Georgia State University

May 2017

DEDICATION

I am dedicating my thesis to my parents and brother, Jean, James, and Jimmy. You have always supported me no matter what I pursued. I started as a kid delivering home medical equipment, became a welder that worked at a machine shop, then became a welding instructor, went back to school for chemistry, and now I am completing my Master's. Thank you for all the times you sacrificed what you could so that I could get this far. It hasn't been a short road, and it surely hasn't been an easy one, but we made it. I love you.

ACKNOWLEDGEMENTS

I would like to give special thanks to my advisor, Dr. Gangli Wang, for allowing me to come into his lab and learn what I could with the time I had there. He always pushed the importance of efficiency and demonstrated on many occasions how to become more efficient as a worker and person. I have learned much from him and the skills learned will benefit me wherever I go, and for this, I am thankful.

I would like to thank my committee members, Dr. Ming Luo and Dr. Ning Fang for their time and attention they provided me.

Much thanks for my lab mates Maksim (Max) Kvetny, Warren Brown, Jonathan Padelford, and Yan Li for helping me through this project. Thank you, Yan, for suggesting that I pursue this, thank you, Max, for withstanding my crazy line of thinking and bringing me back to Earth, thank you, Warren, for being there whenever I had a question or needed help, and thank you, Jonathan, for keeping me sane. And I thank the rest of the lab for being there to lend an ear and make the days more fun.

Finally, I would like to thank my family and friends once more for helping me through this whole experience and supporting me. If I ever needed anything, it was provided. My friends made me go out and paid my way when money was non-existent. It means the world to have this kind of support from you.

TABLE OF CONTENTS

LIST OF TABLES

LIST OF FIGURES

1 INTRODUCTION

One of the first experimental attempts at protein crystallization happened in 1840 by Hünefeld; using earthworm hemoglobin.[1-3] Crystallizations have been carried out on variations of hemoglobin, enzyme pepsins, viruses, and other proteins. Protein crystallography is important in providing structural information, which can provide insight into the function of various enzymes and other proteins. Crystallization of proteins also is critical in drug discovery since the macromolecule structure provides a better understanding of the possible target binding site.[4-6] The quality of the crystals will determine if structural information can be obtained through X-ray crystallography. Along with providing information about a protein, protein crystallization is used for purification and delivery of many pharmaceuticals.[2, 4-6]

Although much has been accomplished using protein crystallization, there is a lack of active control of the dynamic heterogeneous process as well as lack of fundamental understanding at molecular level or from bottom-up perspective (in comparison to ensemble averages). The techniques used to crystalize a protein can be time intensive and require large excess samples to explore various conditions. There are general strategies to accomplish protein crystallization, but the control of when and where a crystal will form and whether crystallization will occur is difficult or unpredictable. This tends to be the bottleneck for obtaining quality protein crystals.[7-10] Protein nucleation corresponds to the transition from a homogeneous protein solution to the formation of an interface of a nucleus or molecular assembly. The mechanism of this heterogeneous process that leads to a crystal formation needs to be studied so that it may be understood and eventually be controlled. Localizing an environment that a single process be monitored is one of the first steps to address the heterogeneity problem. The next is a

method/tool that is capable to monitor the molecular nucleation that ultimately transforms into a crystal. The final step is to induce transformation actively.

Unfortunately, current technology for crystallization has limited special control to create a localized environment comparable in dimensions to a nucleus so that individual events can be monitored and eventually be triggered. The best techniques for trying to localize the environment use micro/nanofluidic systems.[11-16] Nanofluidic systems use nanoliter volumes that get dispensed rather than microliter. These devices are able to use less volume and test more conditions than the conventional techniques. As of today, high throughput methods have been developed to increase the probability of crystallization.[12] These high throughput methods are better than conventional processes; however, these still screen a variety of relevant parameters, trial-and-error or systematic. High-throughput processes generally use small multi-well devices to test crystallization conditions in parallel and save time, but still do not offer any more control than previous techniques and inherently have low efficiency.[12] None of these techniques or methods provides information involving the location of crystal formation, when a crystal will form, or the ability to control the rate at which a crystal will grow at an individual level.

Crystallization, can be divided into two sequential processes in general – initial nucleation and growth.[17] Nucleation is the formation of a particle larger than the critical size. Critical size is the minimum size of particles that come together to make a new phase, and this formation is called a nucleation. There is an energy barrier that must be overcome for nucleation to occur.[2, 7, 10]

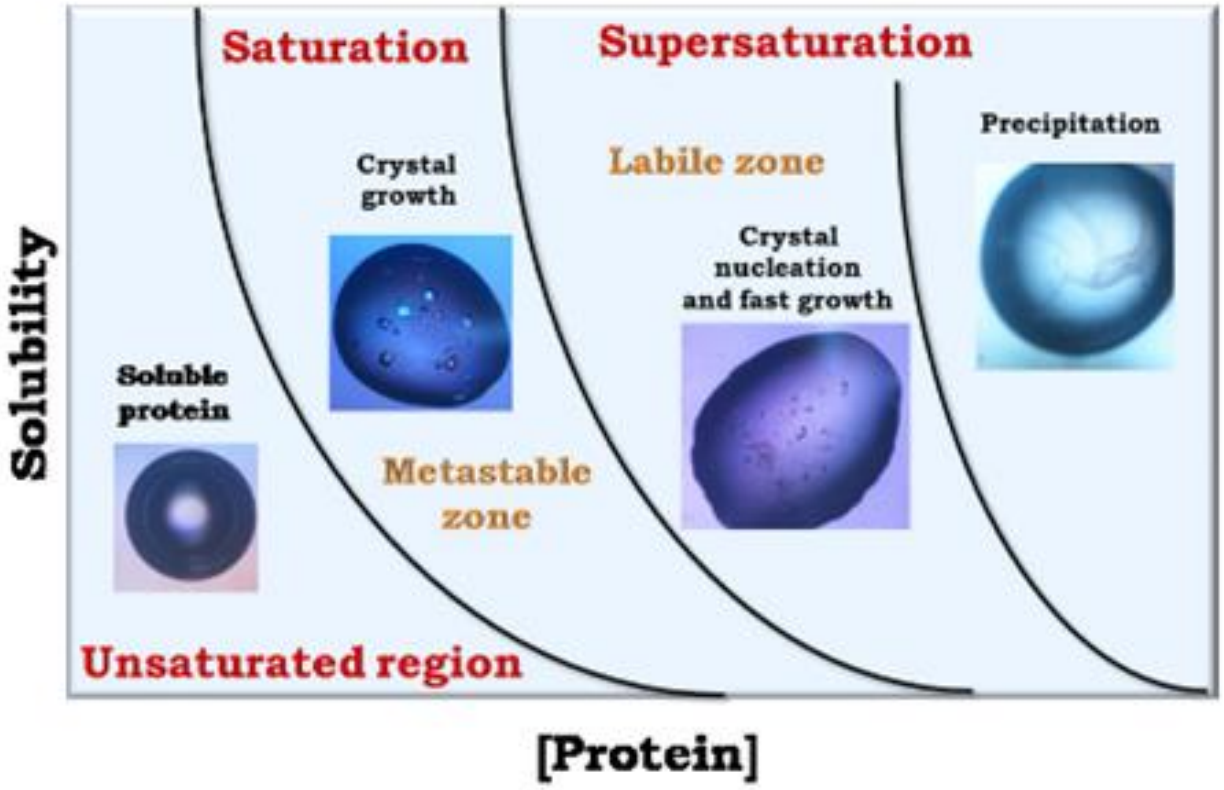

Figure 1-1 Schematic solubility curve for a protein, as a function of the protein concentration[17]

As shown in Figure 1.1 a common strategy to induce nucleation is to have the protein solution within the labile zone but very close to the boundary of the metastable zone. Once a nucleus forms, the protein concentration decreases and brings the system into the metastable zone.[17-19] The metastable zone is ideal for slow crystal growth and has shown to produce the best packing. Nucleation cannot occur in the metastable zone.[17-19] However, nucleation and growth can both occur within the labile zone, but this produces poor quality crystals due to bad packing.[17-19] Crystals will grow in the precipitation zone, but nucleation happens quickly and produces disordered structures and a lot of precipitates.[17-19] Many methods are used to produce crystals, but none actively induce crystallization. Hanging drop, sitting drop, microdialysis, etc. are all

passive methods. To control crystallization and have a higher rate of success an active system must be created.

Having a system that can actively nucleate may be possible by the application of a potential bias or current to the system. By applying energy to the system via current clamping or voltage clamping the energy barrier can be overcome.[17, 20-23] The small opening of a nanopipette can be used to localize this nucleation process. By applying an electrical bias through a nanopipette, this triggers single nuclei formation at the tip of the nanopipette. An electrical response can be monitored along with an optical observation. The signal can then be analyzed to determine the moment of nucleation.

Insulin was chosen for our experiments because the system has been studied for a long time and is well understood. Having a protein system that is already well understood is ideal for establishing a new method. Studies have shown that different morphologies have different pharmacokinetic benefits.[24-27] Main differences in the pharmacokinetics of insulin are amorphous drugs dissolve quickly but provide short-lasting effects, and crystalline forms of insulin dissolve slowly and have longer lasting effects.[24, 28] Crystal size distribution in the drug is critical for treatment.[29] It is necessary that crystals are larger than 10 μm to ensure long lasting effects of the drug; however, they need to be smaller than 15 μm to avoid clogging when using a fine needle for injections.[30-31]

A single nanopipette is used to initiate nucleation and crystal growth in an analyte solution at the metastable zone. By preparing an insulin solution within the metastable zone, we are able to avoid spontaneous nucleation that will occur in the labile and precipitation zones and often produces poor crystal quality if left conditions stay inside that zone for too long. The metastable zone is suitable for crystal growth but not the formation of a nucleus. This provides an

environment ideal for inducing nucleation through an external stimulus, such as an applied current or potential. Since the system is controlled externally by an electronic device, transport of ions/charges or disruptence of the ion transport generates electrical responses that can be measured and recorded in real time. To localize the nucleation and growth of the crystal, we use a nanopipette. This allows one to observe the formation of a crystal via a microscope. The electrical response measurements along with real-time visual observations make it possible to study nucleation and crystal growth.

2 EXPERIMENT

Instruments:

P-2000 nanopipettes puller, Sutter Instrument Co.

Quarts Glass Capillary with Filament, O.D.: 1.0 mm, I.D.: 0.7nmm, 7.5 cm length, Sutter Instruments Co.

Gamry Reference 3000, Gamry Co.

Axon Molecular Devices

Axopatch 200B

Digidata 1440A

Olympus Microscope, Dino-line eye eyepiece 1.3 Mp Camera

Olympus BX51WI Microscope

Preparation of Nanopipettes:

Pulling the nanopipettes uses a 2 step pulling parameters and are as follows:

Pipette Radius (nm)	Heat	Filament	Velocity	Delay	Pull
200	750	4	55	180	80
	700	4	60	150	120
150	750	4	55	180	80
	700	4	60	150	150
80	750	4	55	180	80
	700	4	60	150	180
65	750	4	55	180	80
	700	4	60	150	120

Table 2-1 Pipette pulling parameters for different sizes. This is a table of different pipette sizes and their pulling parameters. All of the programs are 2 line programs.

The pulled nanopipettes are then filled with 1 M HCl and are centrifuged for 10 min at 4600 rpm. However, concentration of HCl may vary depending on experiment.

Chemicals:

Bovine insulin was purchased from Akron Biotech without additional purification. ($ZnCl_2$: Sigma-aldrich/10g, Anhydrous Citrate Acid, Sodium hydroxide pellets, J.T.Baker, Hydrochloric Acid: Fisher Scientific)

Preparation of Insulin Solution:

10mg Insulin was dissolved in 8mL 0.02 M HCl. Then 1mL of 0.1M $ZnCl_2$ and 1mL 2M Citric Acid was added to the solution. The solubility of insulin is pH dependent with a PI around pH 5.4. The pH of the 5mL solution was adjusted by adding 8M NaOH until it formed a white cloudy solution, and continued adding 8M NaOH until the white cloud dissipated at which point

the solution is adjusted to pH 7.9 using 6M HCl. The solution[4-5] can be adjusted later on to test different pH solutions.[32-33]

To fine-tune the solution pH, 200μL aliquots of insulin solutions at different pH were prepared. The solutions were monitored for the next 24 to 48 hours. The more hydrochloric acid added to the solution, the faster microseeds formed. The solution that did not form crystals within 24 hours but has the closest pH to the solution that did crystalize is the solution that is used or experiments. The goal is to create an insulin solution that is in the metastable zone with an appropriate lifetime without spontaneous nucleation.[32-33]

Experimental Setup:

A glass slide was made using ITO glass as the electrically conductive platform, and non-conductive glass pieces are attached to the ITO surface to act as a guide for the nanopipette. Melted wax was applied to the surface and shaped to form an area that the protein solution could be contained in. This allows the nanopipette to be guided into 50 μL of protein solution and secured so it does not move during the experiment. Vacuum grease is applied to the top surface of the wax so once the glass slide cover is placed on top, it creates a seal to prevent evaporation of the protein solution along with a surface that is appropriate for use with a microscope.

Once the pipette is placed on the slide containing solution, the working electrode made from silver wire is inserted into the nanopipette containing 1 M HCl and the reference is connected to the surface of the ITO glass slide, see figure 2.1.

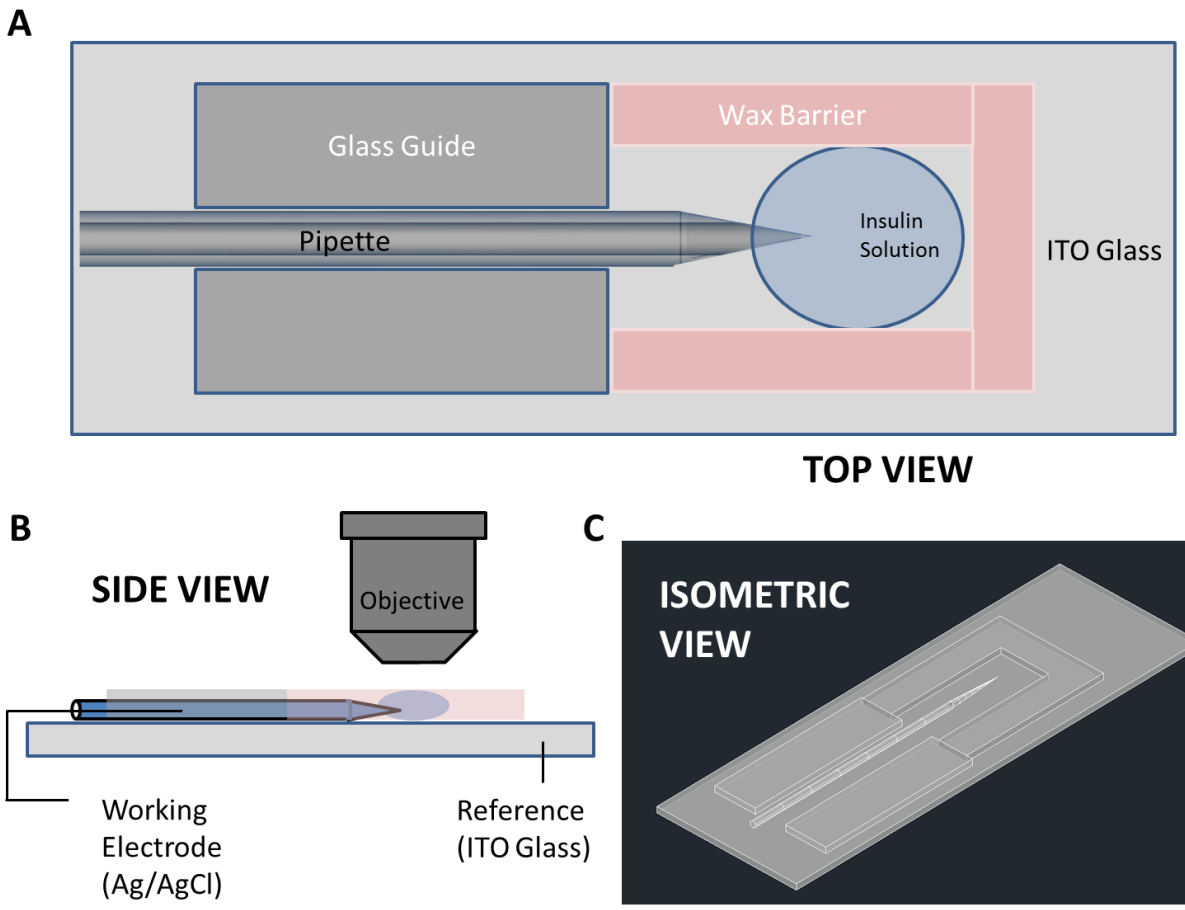

Figure 2-1 Experimental Setup and the device at different views. a) Top view displaying how the glass channel guides and holds the nanopipette in place. This view also shows the wax walls that contain the insulin solution, which also has a glass coverslip placed on top. b) Side view that displays the nanopipette laying on the ITO Glass slide with the tip inserted into the protein solution that is being contained by the wax wall. Image B also shows the Ag/AgCl electrode inserted into the nanopipette which is the working electrode in the experiment and the ITO Glass slide is being used as the reference. c) Isometric view to provide a better 3 dimensional representation of what the device actually looks like.

Figure 2.1 shows the device and the experimental setup for nucleation at different point of views. Figure 2.1 A is the top view of the device used. This shows the glass guides that holds the nanopipette in place to prevent moment during the experiment that would damage the nanotip. It also shows the wax walls that are used for containing the insulin solution droplet, along with how the nanopipette inserted into the solution. In a later model, the wax walls were

replaced with a glass wall barrier that was made by using a square piece of the glass slide. The center portion of the glass piece was ground out using a die grinder with a diamond bit. This created a solid piece with an open section for solution to go into.

Figure 2.1 B shows a side view of the device, which shows the nanopipette inserted into the insulin solution. The image also shows the working electrode, made out of 0.18 mm Ag/AgCl wire, inserted into the glass capillary filled with hydrochloric acid. It also shows the ITO glass slide acts as the reference electrode. This figure also demonstrates the microscope setup with the objective positioned over the protein solution to monitor what occurs at the tip under bright field.

Figure 2.1 C is the isometric view of the device. This is just a 3 dimensional view of the device. This shows the ITO glass slide platform, along with the glass guides to support the nanopipette being inserted into the bay containing the protein solution. It also shows the wax walls that acts as a barrier to contain the protein solution.

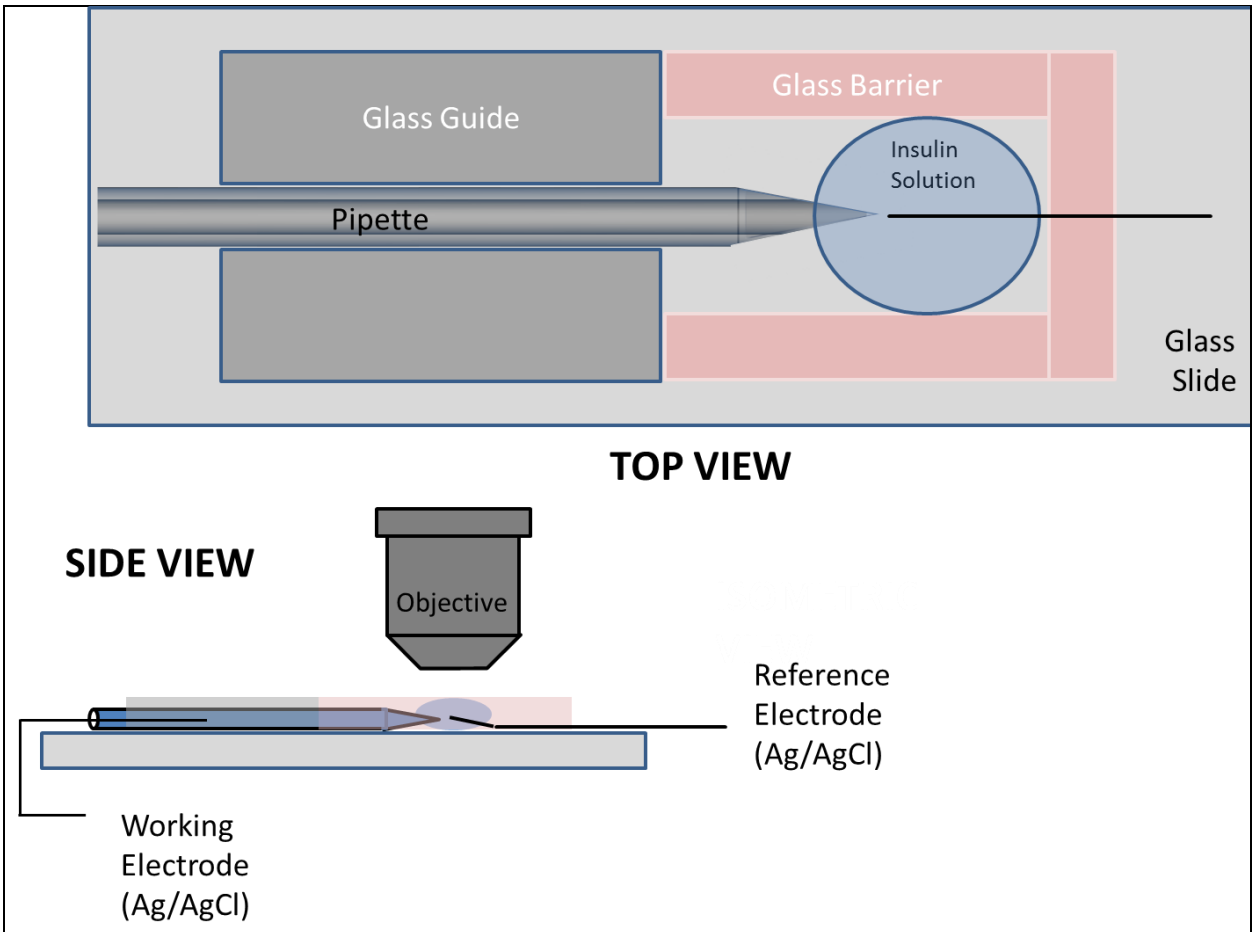

Figure 2-2 Point Field Device Setup. This is a modified device that is used for point field experiments. The top view shows a device that instead of using an ITO glass slide platform, this device uses a nonconductive glass slide. Another change is a glass wall barrier is made to place on top of the glass slide platform, instead of having a wax wall. This new devices uses an Ag/AgCl reference electrode. The side view shows the point field device and how the Ag/AgCl reference electrode is positioned.

Figure 2.2 shows the setup for the point field device. A point field device is meant to have the reference electrode close to the nanopipette tip to avoid applying a uniform field around the tip. It should be close enough to apply a field at only a small area of the tip which creates an unevenly distributed field on the tip. It is split into two views: top and side. The top view shows the device shows a bird's eye view and how the components are positioned on the ITO glass platform. The device is similar to the device in figure 2.1; however, critical components have

been modified. The platform is no longer ITO glass, but instead using a nonconductive glass slide. The glass guides are the same and attached using melted wax, but the wax walls are not applied. Instead, a glass slide is cut to make a square. The square glass piece is then modified by having a channel cut into it. This channel will be used to contain the protein solution. The reason for doing this modification is the wax walls eventually deform and breakdown. The deformation is due to using ethanol as a cleaning agent for the glass slide or excessive pressure while cleaning with a kimwipe. Eventually, the deformation and breakdown of the walls affects the performance of containing protein solutions and makes experimentation extremely difficult. To prevent this problem, a glass wall is created and used. To carve out a channel, a die grinder (dremel tool) with a diamond bit was used. **Note: Take extra precaution while performing this task. It is very dangerous and produces glass dust. The glass is extremely delicate and could shatter. Ideally, safety glasses and a clear face shield should be worn. Have a vent near this work to pull the dust or perform in the fume hood.** Also, the last modification is using a new reference electrode made from Ag/AgCl wire. As the side view shows, the Ag/AgCl reference electrode is moved closer to the tip of the nanopipette by being bent upward.

Once the physical device setup is completed, current or voltage can be programmed and applied/collected as shown in figure 2.2. The program can be configured to apply both negative and positive values of current (nA) or potential (mV) along with an adjustable preconditioning, hold, ramp period, and target values.

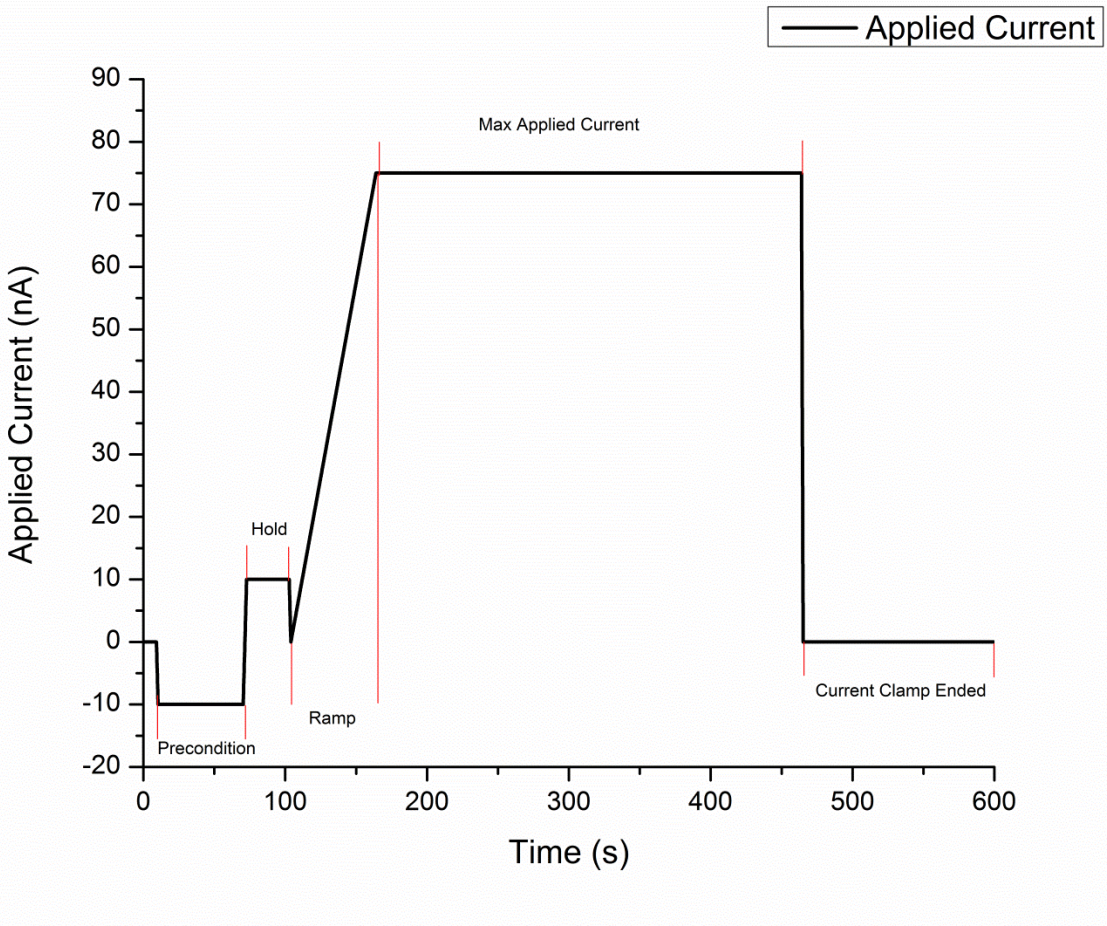

Figure 2-3 Example of Current Clamp mode with different stages of experiment programmed. The figure shows a current clamp experiment and the parameters that can be implemented into an experiment. Both the amplitude and duration in each step can be systematically varied within instrumental hardware limit. This does not mean every step has to be implemented into an experiment.

Figure 2.3 the precondition step is the period where a current is applied to calibrate the experimental conditions and/or prevent uncontrolled formation of a black spot at the end of the pipette during the time needed for physical device setup. This condition can be a negative or positive bias and/or can have a waveform e.g. sine, square, triangular. Hold period is the duration in which a constant current is applied before ramping to the maximum current value. This hold period current can be varied, in this case a 10nA bias is being applied for 30 second. The Ramp

segment is a period where the bias is increased to the maximum applied current set. This ramping time can be changed so that the experiment can have a long ramp time such as (600 seconds) or a short ramp time i.e. (60 seconds). The ramp was used to induce slower transitions of flux at the end of the tip as an optional step. In some experiments, the ramp process caused an adverse effect. In other words, not all experiments were configured to use a ramp. Slowing the formation at the end of the tip sometimes is not desirable in some experiments that the goal is to shock the system or to quickly form something on the end of the pipette to try to force fast nucleation. The maximum applied current is the current that usually is set for the majority of the experiment. This is the current where we expect nucleation to occur or try to induce nucleation. Once the duration for the max applied current is completed, the system may have a period of time where no current is being applied to the system until the whole experiment is over. This is shown in the area "Current Clamp Ended" on the curve. This segment is after the max applied current duration ends, and the system applies a 0 nA current for the remainder of the experiment. The same process is used for potential clamping.

It needs to be recognized that not all experimental curves collected are as clean as shown in later sections of this thesis. Some display more complex signals, i.e. environmental interference due to either poor shielding or grounding. Some representative features are shown in figure 3.7

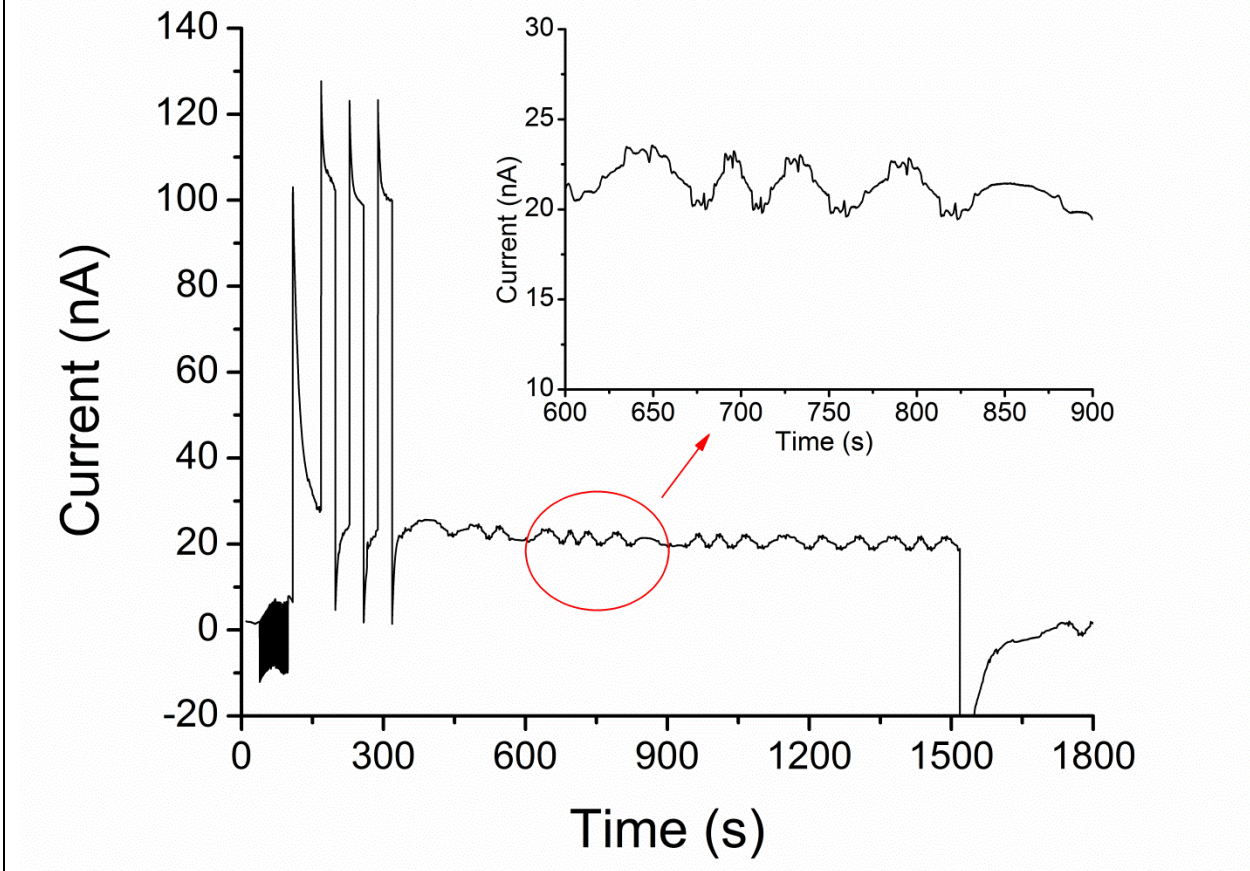

Figure 2-4 Current response curve with poor shielding. This curve is an example of the physical system having poor shielding. Inset highlights the small perturbation in the recorded current amplitude. Data recorded under potential clamping mode with the bias 300 mV and the pulses with a 300 mV amplitude, reaching a peak of 600 mV at the top of the pulse. Using a buffered insulin solution at pH 8.02 with 1 M HCl inside the nanopipette.

Figure 2.4 is a current response curve that shows a periodic current oscillation with small amplitudes in the recorded signal. This is a common problem with not properly shielding equipment when the signal of detection is small (at nanoA). Any other electrical equipment in or near the area of work can affect the signal detected by the system as noise. This can be corrected by using a faraday cage and using proper grounding techniques. However, a problem we noticed

was not having all the cables and wires properly shielded, and after correcting this, we noticed fewer oscillations and better signal quality.

3 RESULTS

3.1 Nucleation

The goal is to induce nucleation and detect it. The basic experimental layout is shown in Figure 2.1. In general, a nanopipette is filled with 1M HCl which can vary depending on the experiment, and inserted into 50μL of the insulin solution that is contained in the home-built ITO chamber. The ITO glass slide is connected as the reference electrode and an Ag/AgCl working electrode is inserted into the capillary portion of the quartz pipette containing the HCl solution. An optical microscope is used to monitor the crystallization process and to record images and video during current and potential clamping.

Diffusion occurs regardless of the applied bias to the system under a concentration gradient. Proton in the interior solution will diffuse into the insulin solution and lower the pH of the exterior solution near the tip of the pipette. This could form what was originally called a black spot while using a 10x objective with the old microscope. With better magnification from the new microscope, 40x, the first optically resolvable structures at the nanotip are referred as spherical to distinguish with the later transformation. Under an applied bias, there will be migration under the electrical field across the nanotip which is controlled via current or voltage clamping. The isoelectric point of insulin is around 5.4 which would make the insulin molecules negatively charged if the pH of the buffered solution is around 8. If a positive bias is applied to the system (inside vs. outside), this would force protons from the hydrochloric acid inside the pipette to migrate out the pipette tip, meanwhile driving the negatively charged insulin molecules towards the tip of the nanopipette. The interfacial zone where the protons and the insulin molecules meet will be different from the bulk insulin solution, as lower pH would establish the

region as metastable or precipitation zones in the phase diagram. Therefore nucleation will be localized near the nanotip as illustrated in Figure 3.1

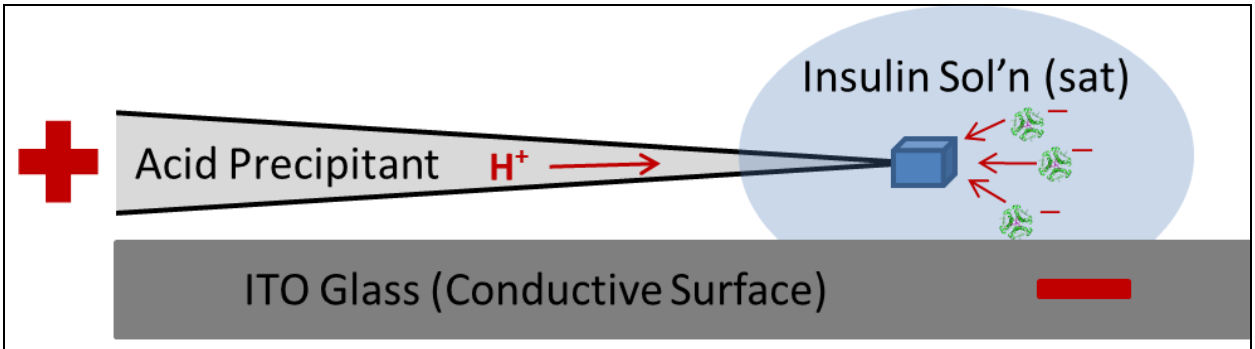

Figure 3-1 Nucleation using Nanopipette inside a ITO Glass chamber. The figure displays how nucleation would occur using the ITO glass and nanopipette filled with an acid precipitant, while using a saturated insulin solution outside.

Using current and/or voltage clamping techniques makes detecting and inducing crystallization possible. In combination with the nanopipette device to localize the environment for nucleation, it is possible to form crystals in a faster and relatively controllable environment. Recently, about 2/3 of the experiments performed formed crystals: out of the last 30 experiments, performed 21 have formed crystals.

3.1.1 Current Clamping

Current clamping is a process in which a current, in most cases in nanoamps range, is held at the programmed values applied to the experimental system while the voltage required to maintain that current amplitude is measured. A programmed current profile is shown in Figure 3.2

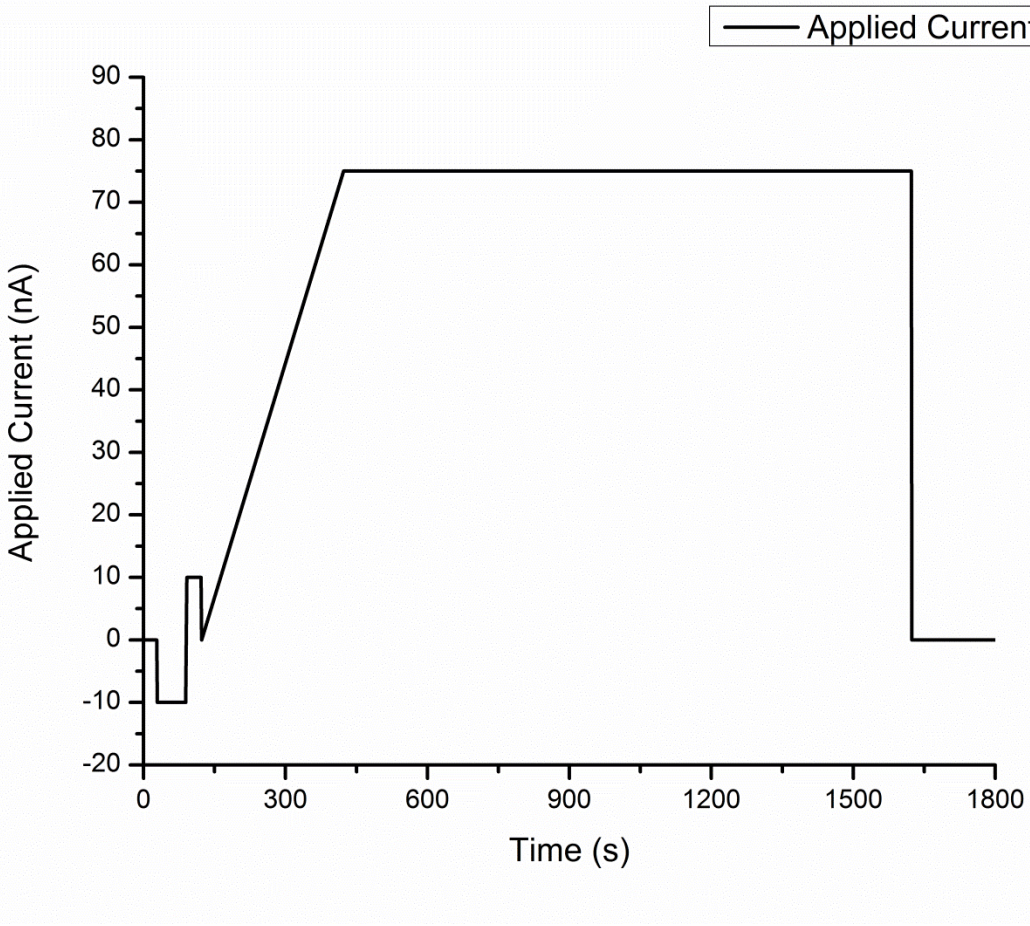

Figure 3-2 Applied current profile in current clamp experiment. The current is applied externally in the current clamp mode by an instrument, which records at the same time the corresponding potential needed, i.e. the potential responses. This particular experiment has a -10nA precondition for 60s, 10nA hold for 30s, and a 300s ramp from 0nA applied current to 75nA maximum applied current for 1200s. The rest of the time of the experiment has 0 nA applied current.

Figure 3.2 has multiple applied current segments at different parts of the experiment. At the beginning of the experiment, there is a precondition at -10nA which is used to prevent or reverse premature black spot formation. Why 10 nA hold? To establish a more constant ion flux before ramping? The system then ramps up linearly to 75nA over a 5 minute period. The reason to slowly ramp current is to control black spot formation and prevent early nucleation. After the system reaches 75nA, the max current, the black spot is formed over a short period that is believed to lead to or indicate nucleation. Current clamping controls ion flux and thus provides a sustained supply of protons to interact with insulin at the nanopipette tip and push the phase diagram toward metastable states and precipitation. The ramp period was originally used to prevent extremely fast nucleation that may be difficult to observe optically at the beginning of the experiment. The ramp is also used to slow down the mass transport so that nucleation can be studied a few minutes after the experiment is started.

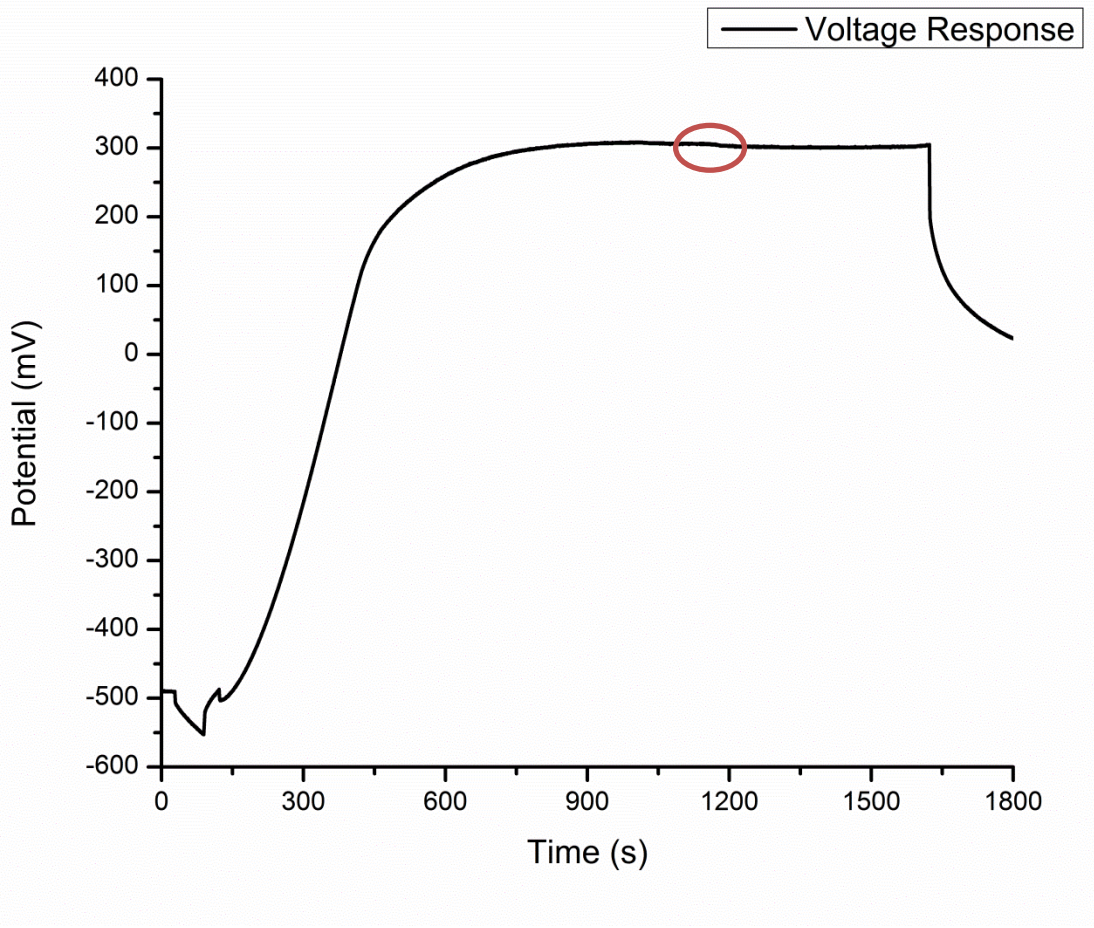

Figure 3-3 Voltage Response Curve. This is the voltage response from the experiment that implemented the current clamp that was applied in figure 3.1. This particular experiment has a -10nA precondition for 60s, 10nA hold for 30s, and a 300s ramp from 0nA applied current to 75nA maximum applied current for 1200s. The rest of the time of the experiment has 0nA applied bias. At the maximum applied current the potential is about 300mV.

The potential, measured in millivolts, is the electrical signal being measured in the system. Figure 3.3 shows the measured potential responses corresponding to the precondition, holding, ramping, and maximum applied current as defined in Figure 3.2. The goal is to identify if a signal in the voltage response curve could predict or correlate with a visual change monitored by the optical microscope. The assumption is that formation of a heterogeneous structure near the nanotip would disrupt the ion flux and generate a detectable electrical signal. Ideally, the

signal will be in the region of the plateau in the voltage response so that a better-defined baseline exists. It is difficult to identify such features during the ramping period when more significant changes occur. In this experiment, there is a feature in the plateau region as shown in Figure 3.4.

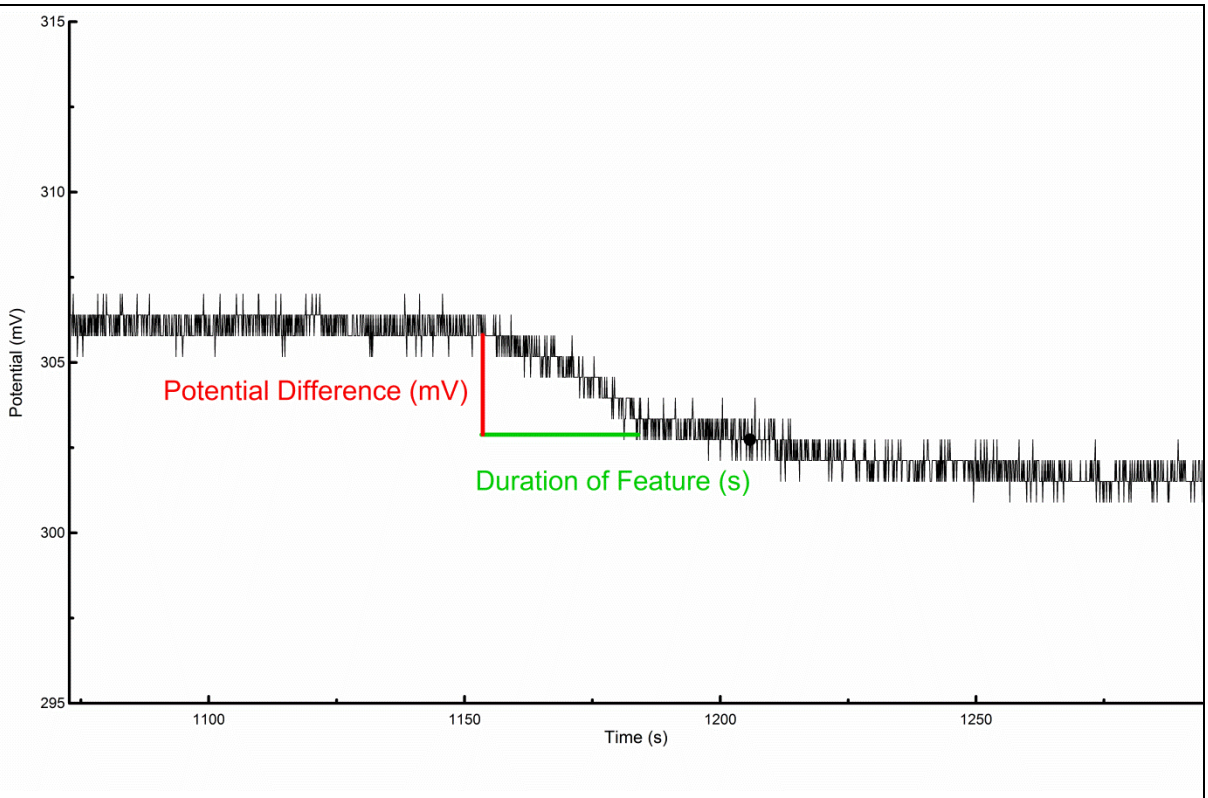

Figure 3-4 Potential variation corresponding to transition from spherical structure to non-spherical structure. This graph displays a voltage response during a current clamp experiment that indicates disruption of ion flux.

Figure 3.4 shows a voltage decrease during which a physical change is observed optically under the microscope. In this case, there is a decrease in voltage in a short period. The total decrease is measured in millivolts while the duration of the feature is measured in seconds. It is normal to see a deviation of the voltage of this magnitude throughout an experiment. Therefore, at this point, the illustrated feature cannot be concluded to indicate any structure formation. However, such sudden changes are different from baseline drift or random noise, as shown in the other part of the curve, and thus believed to be promising indicators that a physical change may

be occurring at the tip, such as a tranformation. Additional measurements and analysis are required to validate or confirm. The feature shows a 4 mV decrease over a 30 second duration. The physical change, monitored through a microscope, at the nanopipette's tip during the time of this feature indicated in Figure 3.4 is shown in Figure 3.5

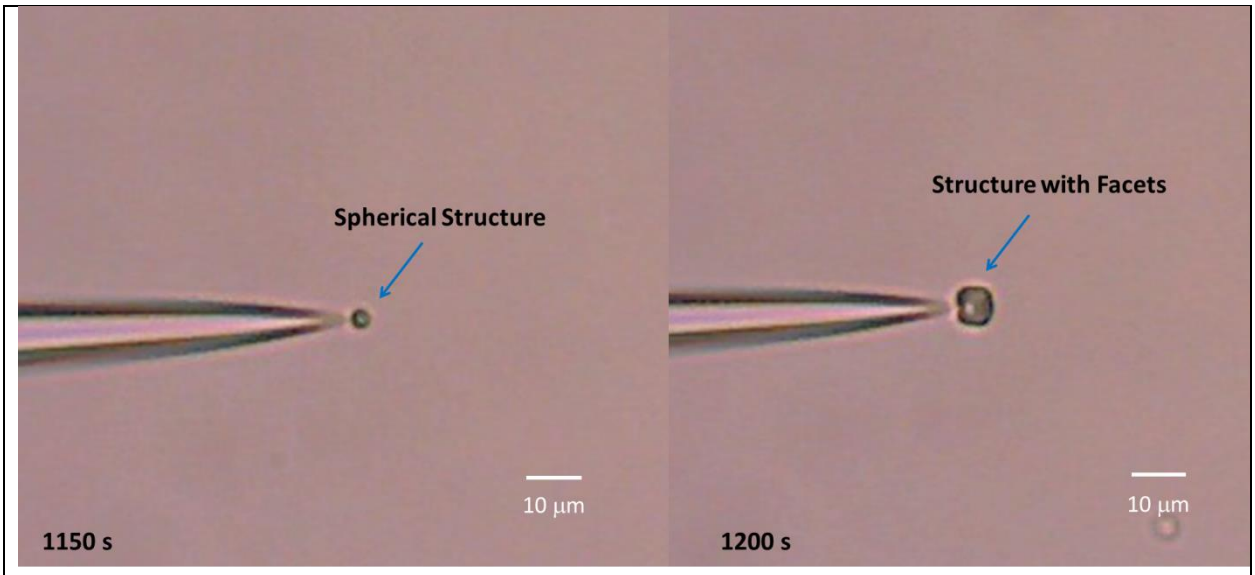

Figure 3-5 Brightfield images of the changes at the nanotip monitored by optical microscope. FigureThe left image is before the voltage drop feature. And the right image is immediately after the voltage drop. Performed with 10x objective, 200 nm pipette, 1M HCl, and 7.9 pH insulin solution

The change is occurring between the left and right images in Figure 3.5 highlights non-spherical structural development. The left picture, taken at 1150 s, indicates a round structure with no lattice structure resolved. The right image is taken after the voltage decreased as shown in Figure 3.4, at 1200 s. Facets can be clearly resolved indicating lattice structure. The physical change takes place over 50 s. The change here corresponds to having a completely round structure to the whole round structure transformed to a structure with facets. Having a round structure with no features such as facets transformed into a structure with facets is a physical

change and a visual indicator of achieving and maybe completing nucleation. The round structure is not yet fully understood; however, the structure does decrease in size when current is no longer applied to the system, or a negative bias is applied. It will be interesting to further characterize this gel-like round structure and correlate to the concept/theory of dense liquid domain that requires experimental evidence.[34-35] The structure with facets, on the other hand, is more solid/robust which does not decrease in size or dissolve when current application is shut off, or a negative bias is applied to the system.

3.1.2 Voltage Clamping

Voltage clamping is a process in which the system applies a potential, either a constant value or with different waveforms, and record the current responses as shown in Figure 3.6 and Figure 3.7.

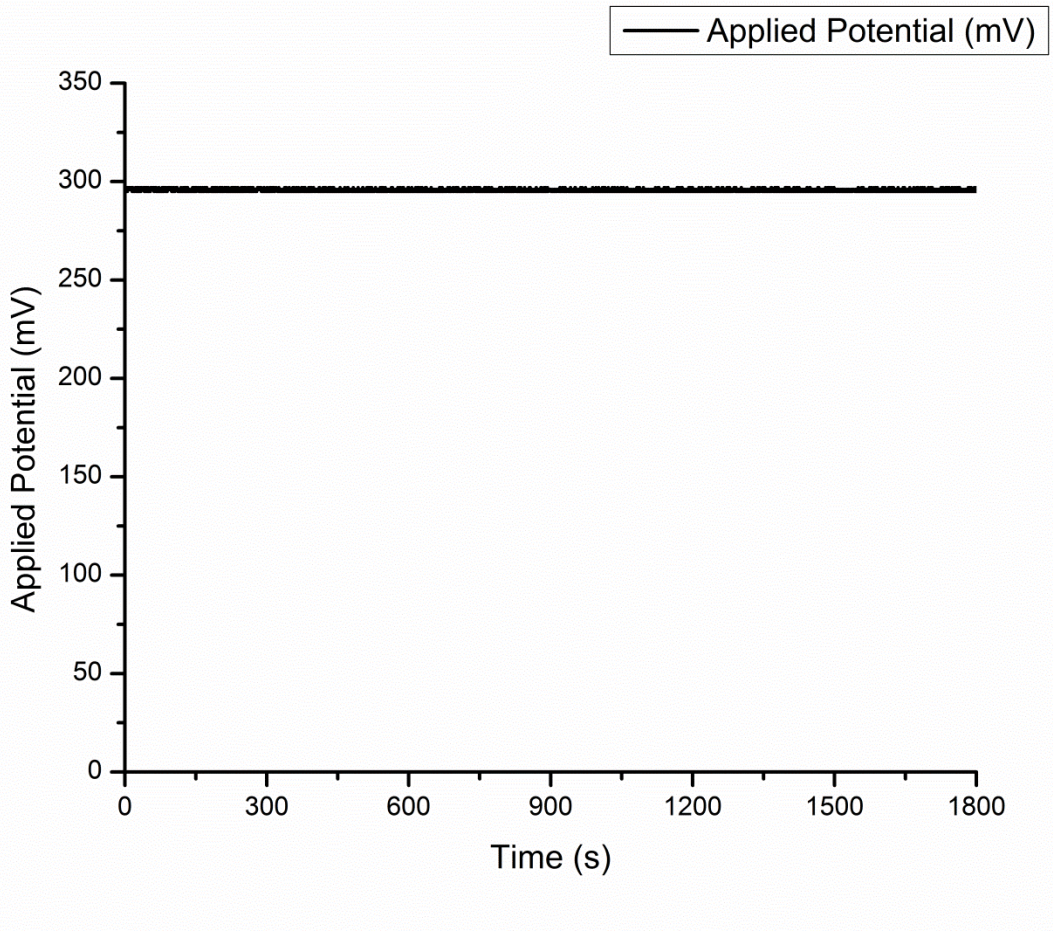

Figure 3-6 Applied Potential in Voltage Clamping. This graph represents the applied potential during the voltage clamping process. In this case a 300mV bias is applied to the system for 1800s then drops to 0mV applied bias.

Figure 3.6 defines a voltage clamp experiment in which there is no precondition, hold, or ramping steps programmed. This system is held at 300mV for 30 minutes. Experiments can vary in time and potential, along with having different steps such as a precondition, hold, and ramp

periods. When voltage is held constant, the force used to migrate ions through the nanopipette is held constant; however, due to concentration of ions decreasing over time, the amount of ions migrating through the nanopipette could decrease. At 75 nA current, for a 75-nm-nanotip containing 5.7 μL 1 M HCl solution, the concentration would drop to 0.01 M over 120 minutes by ion migration.

Shown in Figure 3.7 below, the current response decreases from the beginning of the potential applied in the current response curve. This is due to the charging-discharging of the solution system under any electrical potential variation, often characterized by an RC time constant. This charging current diminishes when the system equilibrates and approaches a steady-state current response, i.e. after about 300 s in this curve. Ideally, one would want the nucleation to occur under steady-state regime. If a transition occurs during the spike, it can be extremely difficult, and nearly impossible, to find the signal response that corresponds to the disruption induced by nucleation.

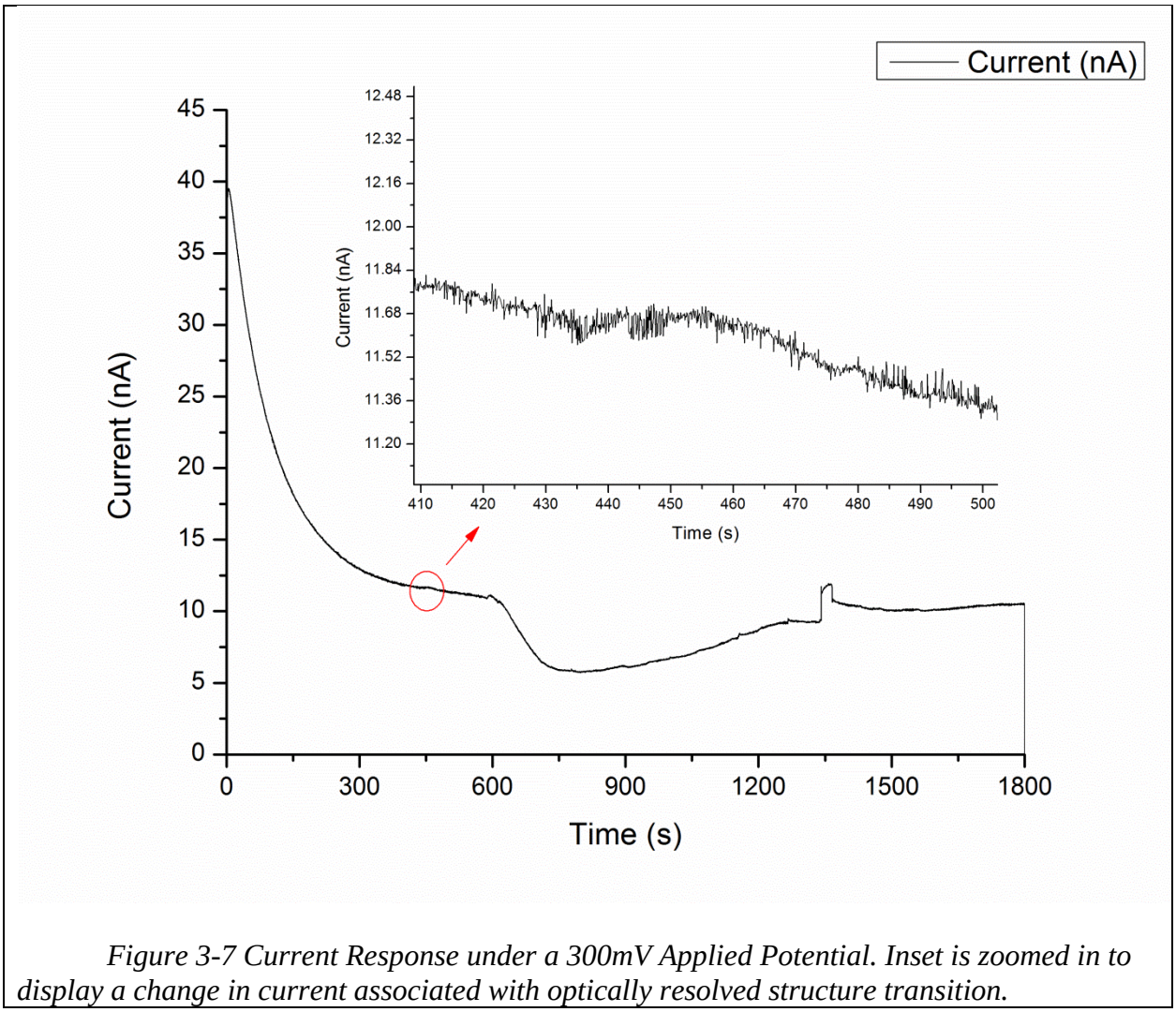

Figure 3-7 Current Response under a 300mV Applied Potential. Inset is zoomed in to display a change in current associated with optically resolved structure transition.

Inset highlights the feature associated with structure development before and after nucleation. In the zoomed in view of the current curve around 430s to about 480 seconds, there is a very weak increase in current of about 0.2nA after baseline correction. Although very small, the corresponding images taken around the same time points reveal the physical changes shown in Figure 3.8

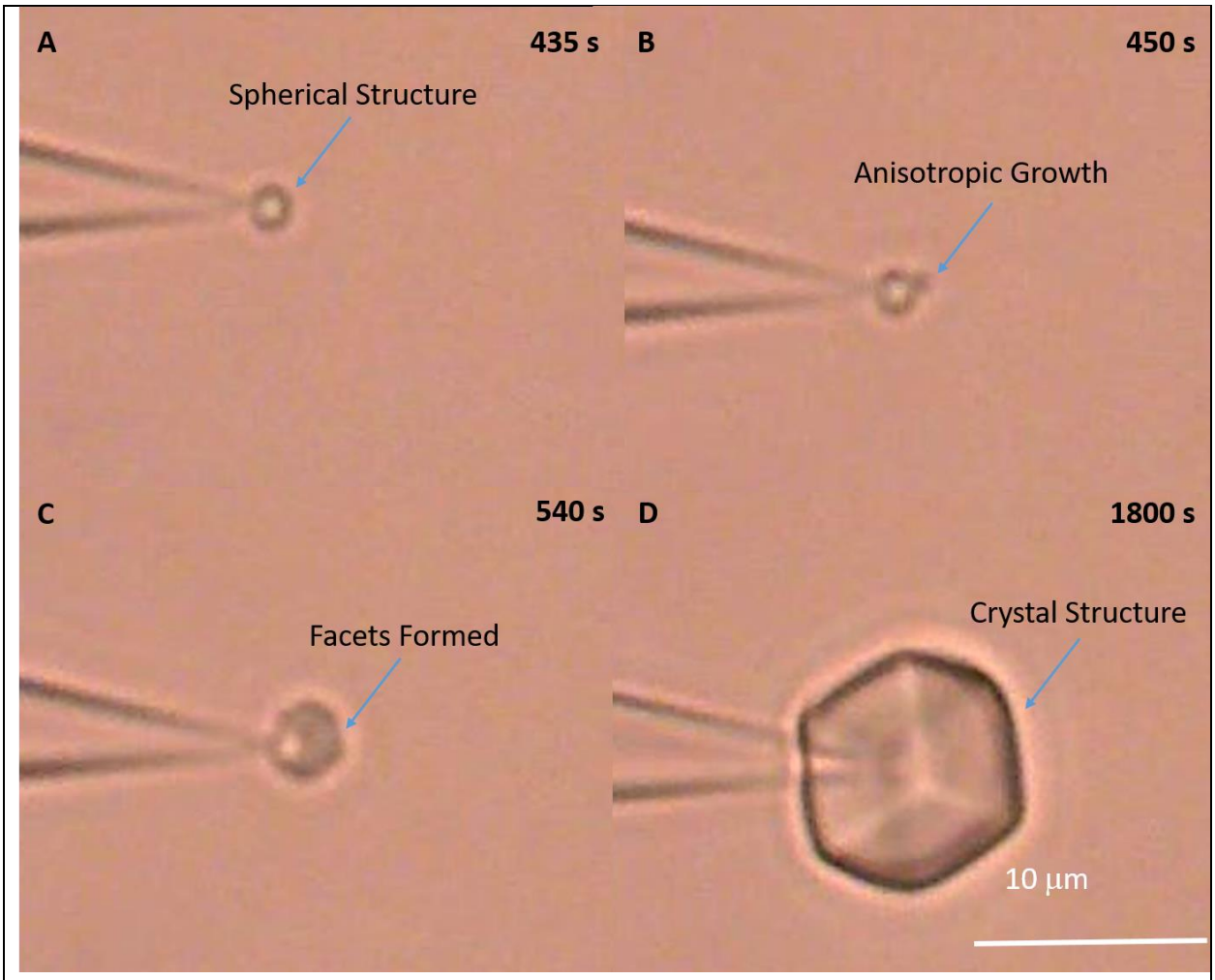

Figure 3-8 Crystal Formation under 300mV Voltage Clamping. These 4 images were taken during the voltage clamp experiment presented in Figures 3.6 and 3.7. Panels A) to D) were taken at435s, 450s, 540s and 1800s after the potential was applied. Performed with 40x objective, 75 nm pipette, 1M HCl, and 8.02 pH insulin solution

Four images are included in Figure 3.8 capturing key optical features during a crystalline structure formation.

Fig. 3.8 A is an image taken at 435 s that shows a formation of a round structure on the tip. There are no facets or structures on the surface of this structure. This is ordinary in a system that has not nucleated. It is worth mentioning that the size of the sphere grows over time. Under a lower bias, it might stabilize at a smaller size and never undergo further structure development.

Fig 3.8 B is an image taken at 450 s and shows a structure forming on the outer boundary of the round structure. If comparing this optical image with the current response in Figure 3.7 at the same time, one will notice an increase in the response curve at the transition from times 435 s and 450 seconds. This increase in current response appears to be associated with the formation of the spot that is on the outer boundary.

Fig 3.8 C is taken at 530 s and displays the spot growing into a faceted structure. It appears that it is transforming the round structure starting from the spot that formed in fig. 3.8 B and moving from that point of origin outward until the entirety of the structure is transformed into a faceted structure.

Fig 3.8 D is an image taken at the end of the experiment, 1800 s, and shows a crystalline structure. This shows clear formation of facets and growth of a crystal within a short period of time.

Therefore, the transition from image A to image B corresponds well with the current changes in Fig. 7 inset, starting time and duration wise. The correlation between both conductivity responses and physical changes through observation through a microscope provides more indications on when nucleation occurs.

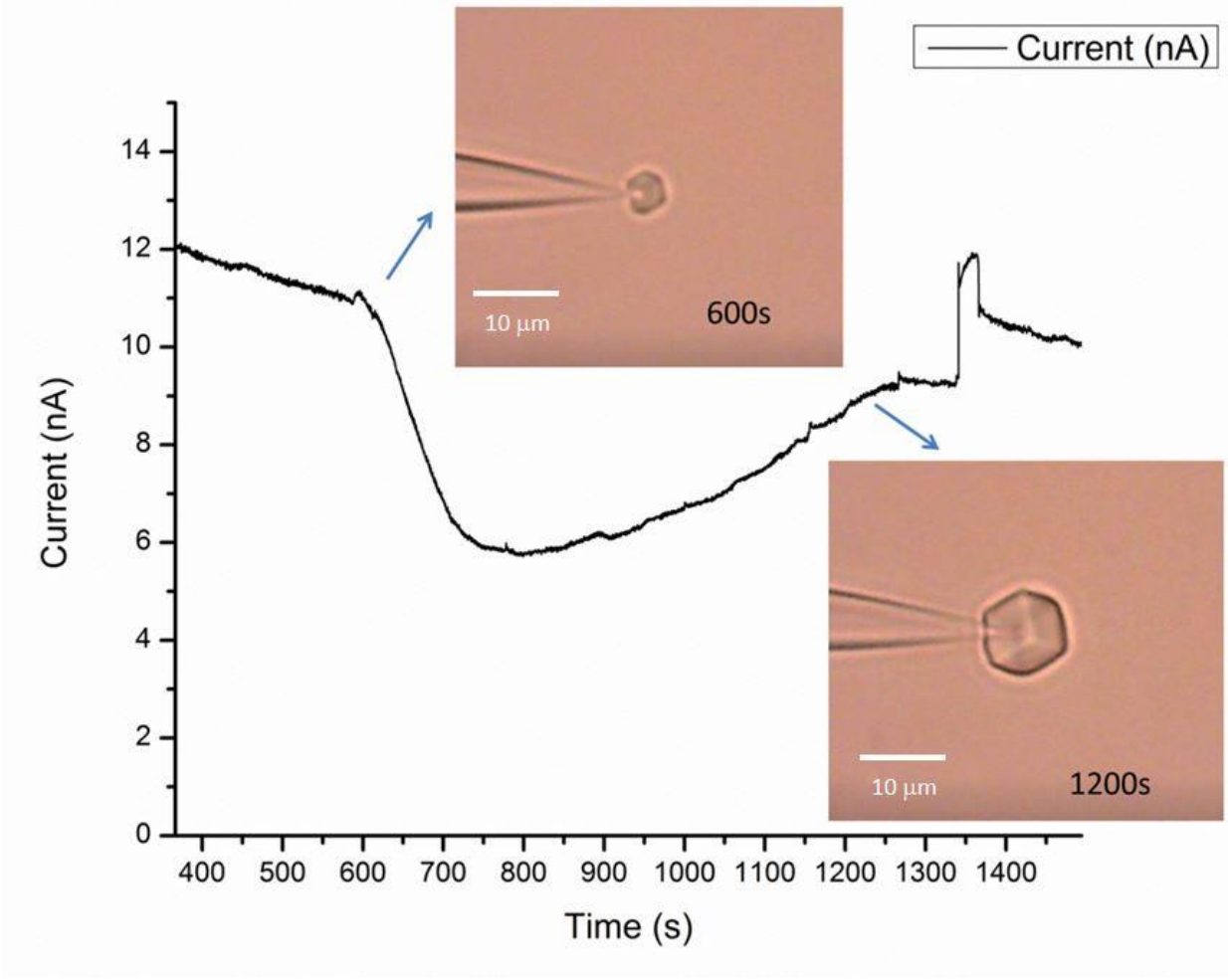

Figure 3-9 Big Current Decrease in Current Response of 300mV Applied Potentia. This figure is showing the large current decrease shown in figure 3.7. It starts at 600 seconds and ends at about 1200s. Pictures of the crystal formation at the end of the pipette are shown at the corresponding times of the decrease in current. Performed with 40x objective, 75 nm pipette, 1M HCl, and 8.02 pH insulin solution

Looking at the current response curve in Figure 3.7, there is a large decrease in current at around 600s, way after the initial anisotropic structure formation. This is believed to be caused by the growth of the crystal embryo that gradually engulfs the tip and reduces ion flux. Additional details are shown in Figure 3.9.

As shown in Figure 3.9 and Figure 3.7 there is a large current decrease. Two images are included in Figure 3.9 showing the crystal growing at the end of the nanopipette before and after

the large current decrease. The large decrease in current is believed to be caused by the formation of the crystal at the end of the nanopipette blocking the opening of the tip; therefore, increasing resistance and as a result decreasing current.

3.1.3 Pulse Induced Nucleation

Overall, the detected electrical signal corresponding to the observed optical transitions are small. It is unclear what triggers the initial anisotropic/asymmetric structure formation under a steady-state type control. It may be better understood and controlled by attempting to induce nucleation via pulse. Our lab has previously discovered that nucleation is achievable using high potentials, but keeping the potential high for too long creates poor crystal quality. It may be possible to induce nucleation with a brief high current or voltage pulse to nucleate and induce a transformation.

Next, a single pulse or multiple pulses within the current clamping or voltage clamping program is introduced to try to induce nucleation. The following section presents preliminary attempts that require more studies that are systematic. The pulse(s) are designed to control when nucleation occurs by acting as a trigger. The number, duration, and magnitude of the pulse can be programmed to vary systematically based on the observed outcome. Also, the waveform can also be altered among triangular or square waves as seen in Figure 3.10.

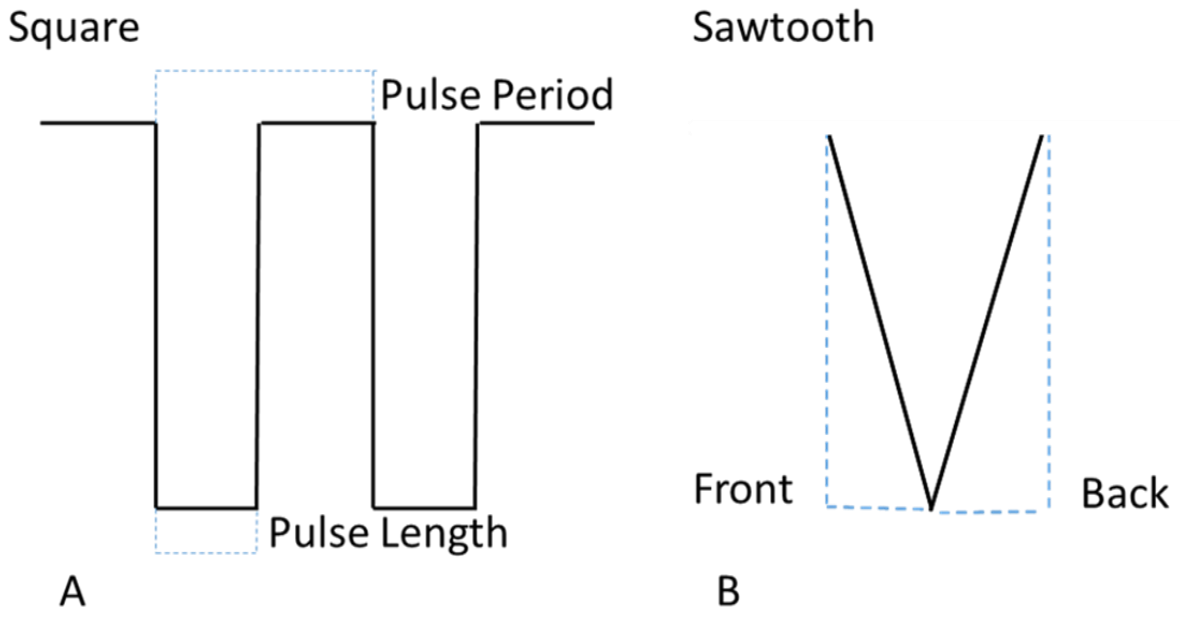

Figure 3-10 Definition of the Pulse waveforms. Along with amplitude, the pulse length the pulse period and amount of pulses can be adjusted independently. A) is a square wave with 2 pulses that shows what the pulse length is and pulse period. B) is a triangular wave, also called a sawtooth depending on how it is adjusted, with a single pulse that shows the other two functions that can be adjusted, the front segment and the back segment.

A square waveform ideally transitions between the maximum and minimum values set in the program instantaneously. In solution measurements, the time constant of the system often limits the switch to about microseconds, which is further lowered in nanopores due to the high impedance. The pulse length is the duration of the applied current or potential at a pulse amplitude away from the baseline. The pulse period is how long the whole pulse is, and this is only meaningful when applying multiple pulses/cycles. The middle panel B is a triangular waveform. The front segment goes from the start of the waveform to the maximum amplitude of the triangular waveform while the back segment is from the maximum amplitude of the triangle wave to the end of the waveform. For a given total duration of the pulse, the durations of the front segment and the back segment can be adjusted so that the front and back segments can be

asymmetric if needed. An example of this would be if the pulse duration was 10 seconds and the front segment was set to 1 second, this would automatically set the back segment to 9 seconds.

Whether the pulse waveform will trigger nucleation is evaluated by the comparison to negative controls. An example would be using either current or voltage depending on the experiment, clamped at a value sufficiently low not to trigger nucleation but also high enough to form a bubble during an 1800s experiment. This will be conducted a couple of times to verify consistency. A negative control is the experiments that do not display a structural transformation, with all conditions the same except the absence of the pulse waveform. After a negative control is conducted, additional experiments are performed with the pulse waveform added to the same parameters used in the negative controls. An example is shown in Figure 3.11 and Figure 3.12.

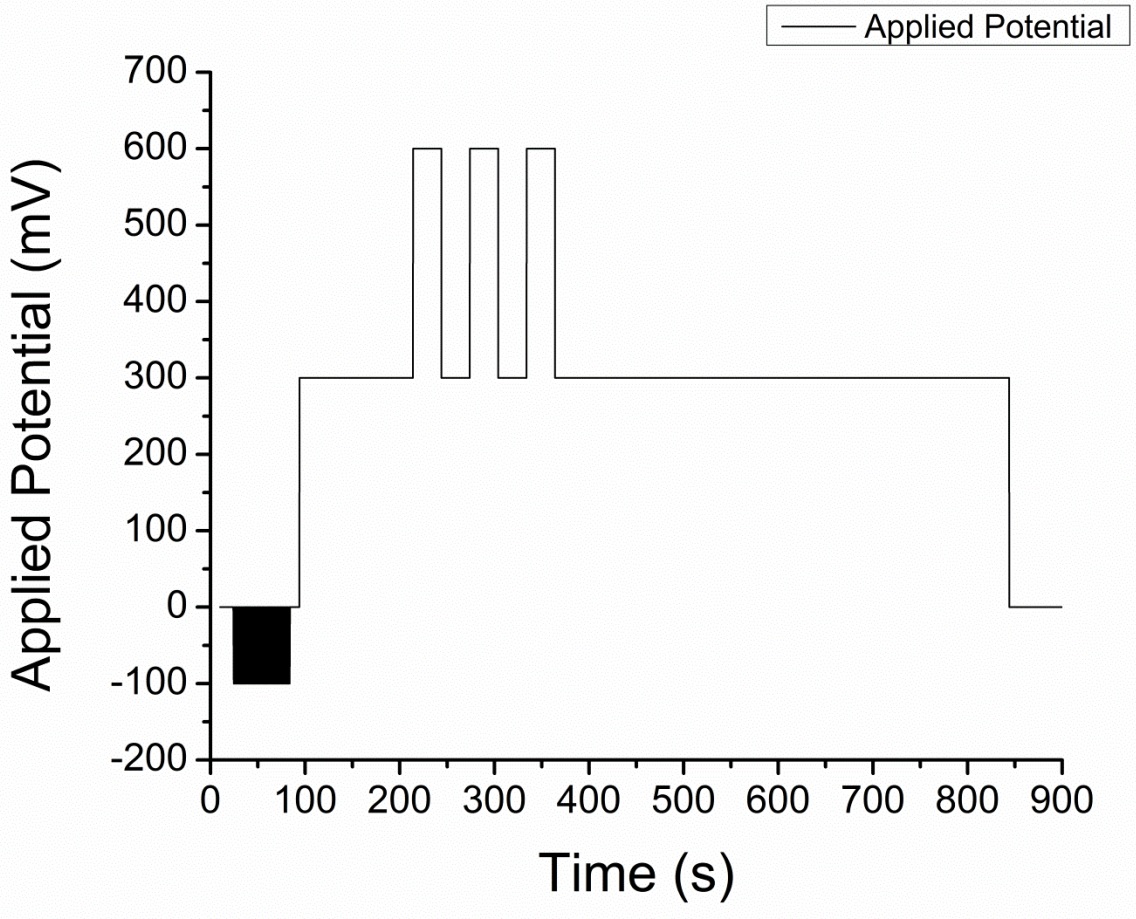

Figure 3-11 Voltage Clamp with Pulse. This is the applied potential for an experiment that uses a pulse to induce nucleation. This applies a 300mV potential for a duration, then applies 3 square wave pulses each 30 seconds long with 30 seconds spacing them apart. Then after the pulses are applied, the rest of the experiment is held at 300mV.

Figure 3.11 is the applied potential curve that displays what is being applied to the system during the experiment. The 300mV application was shown to not nucleate in the negative controls before this experiment; which is why 300mV were used in this particular experiment. 300mV were applied for 120s then 3 pulses were applied, each pulse was 300mV in addition to the 300mV base bias applied, so 600mV total voltage was applied during the pulses for 30 seconds each, and 30 seconds between each pulse. After the pulse sequence is completed, the rest

of experiment is held at 300mV. This produces a current response curve that is used to analyze shown in Figure 3.12

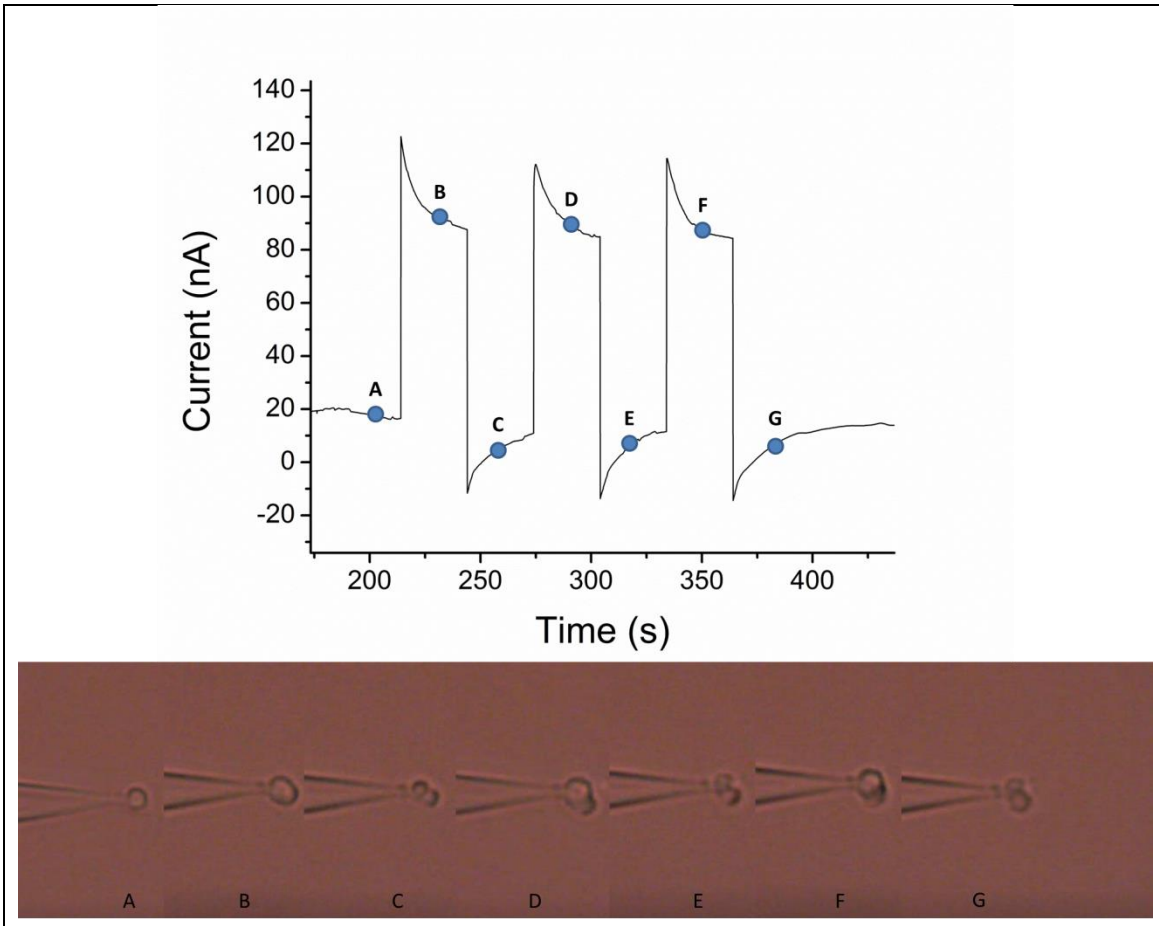

Figure 3-12 Current Response to Voltage Clamp with Pulse shown in Figure 3.11. The images were taken at the corresponding time point shown in the current response. Performed with 40x objective, 75 nm pipette, 1M HCl, and 8.02 pH insulin solution

Figure 3.12 is the current response curve for the voltage clamp with pulse experiment shown in Figure 3.11. This current response displays 3 large peaks where the pulses were applied. The points marked A-G are the points on the current response curve where images are taken from the microscope to observe the physical changes at the end of the nanopipette tip. Point A is taken at 200s into the experiment and is before the first pulse is implemented. It is apparent that there is a spherical structure at the end of the pipette that we are calling a bubble.

There is no feature on the bubble that indicates nucleation occurred. Point B is 230s into the experiment and is during the first pulse which is 300mV greater than the initial potential of 300mV giving a total 600mV potential across the nanopore, which can be seen in Figure 3.11. The image of point B displays a non-spherical structure and now has an oblong shape once the pulse was implemented. Point C is the decrease back to the baseline of 300mV applied potential of the system after the first pulse is completed. The image for point C is at 260s and shows a non-spherical structure; however, it also appears to have two structures connected or maybe a facet that has formed. It should be noted that structures that are non-spherical and have an edge or oblong shape do not dissolve into solution when the electrical bias is turned off. They are structures that are stable in the protein solution environment. Point D within the second pulse, and the potentials are the same as the first pulse. The image for point D, at 290s, displays an increase in size for the structure closest to the tip of the nanopipette. Point E is after the second pulse is completed and back to the baseline potential of 300mV and the image for this point shows the structure decreased in size; however, is larger than in point C. These are a growth of amorphous structures. Point F is the third and final pulse in the sequence and has the same conditions as the other two pulses. The image for point F shows another increase in the size of the structure closest to the nanopipette tip. Finally, point G shows a decrease in current response and the image shows the decrease in a size change.

Deformation of the spherical structures is a promising start point to employ a pulse to initiate nucleation and facet growth. The spherical structure is not a stable structure and will dissipate when external electrical bias is shut off in the system; however, the non-spherical structures that develop do not shrink when external bias is shut off. The images do not show an ideal crystalline structure; however, the pulses did induce a change and if better controlled, might

lead to an induced formation of an ideal crystal. Figure 3.13 below shows a crystal with facets forming using a pulse sequence similar to that used in Figure 3.12

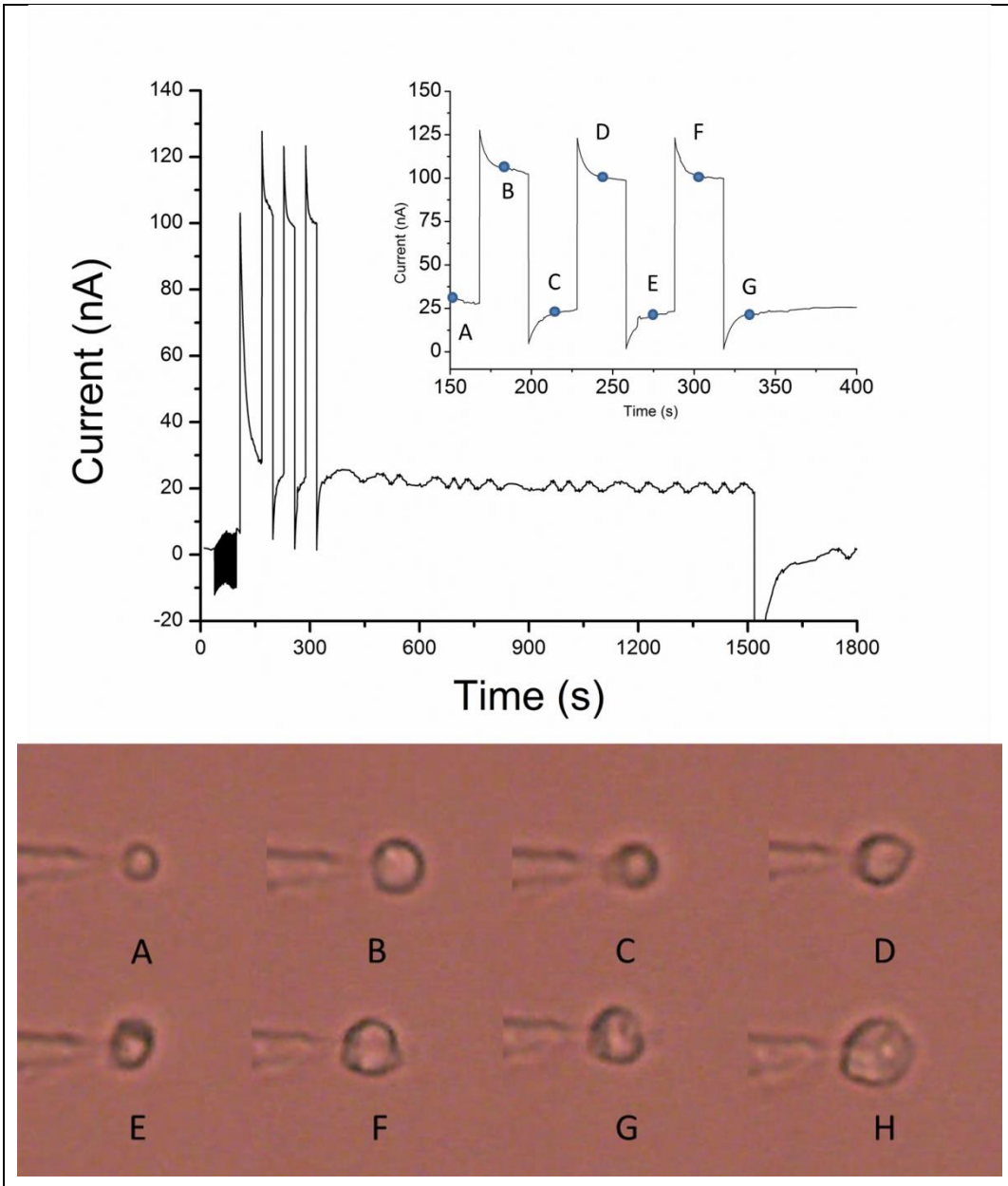

Figure 3-13 Current Response to Voltage Clamp with Pulse and clear nucleation. The top image is of the current response to the voltage clamp with a zoomed in image of the pulses and the spots where pictures were taken of the tip of the nanopipette and what formed on it. Performed with 40x objective, 75 nm pipette, 1M HCl, and 8.02 pH insulin solution.

Figure 3.13 is another example of triggering nucleation using pulses. This shows a similar experiment conducted in Figure 3.12; however, the pulses in Figure 3.13 were applied 60 seconds after the initial application of 300mV of potential were applied instead of 120 seconds after the 300mV application in Figure 3.11. Images A through G in Figure 3.13 show similarities to the images A through G in Figure 3.12 that during the pulse, increased potential, would increase the size of the bubble or object that formed at the end of the nanopipette and would decrease size after the pulse was applied and the potential decreased back down to 300mV. The difference between the sets of images is that the result, image H, of Figure 3.13 is a single object that has visible facets forming indicating crystal formation, while image H of Figure 3.12 has multiple structures that are more amorphous.

After conducting many experiments, the square waveforms had more consistent results with forming something, crystal or amorphous structure. The triangular and sawtooth waveforms did not form crystals or amorphous structures. It is not yet conclusive which pulse parameters induce better crystal structures, but it is possible to induce a formation at the end of the nanopipette tip.

		Pulse Train						Growth Period			
Experement	Clamp	Magnitude	Wave Pattern	Pulse Direction	Pulse Period (s)	Pulse Length (s)	Pulse Count	Pulse Amplitude	Amplitude	Durration (s)	Notes
Crystalization	i	80-180 nA	Square	Down	N/A	30-60	1	0-20 nA	20-30 nA	1500	1/5 crystals
Crystalization	i	110 nA	Square	Down	5 - 40	2 - 10	1 to 5	0-20	30 nA	600	More Pulse = Higher chance of forming
(-)	i	20-30 nA	N/A	N/A	N/A	N/A	N/A	N/A	N/A	N/A	No crystal
(+)	i	80-120 nA	N/A	N/A	N/A	N/A	N/A	N/A	N/A	N/A	Crystals
Crystalization	V	300 mV	Square	Up	N/A	60-600	1	600-900 mV	300 mV	120 - 900	2/5 crystals
Crystalization	V	900 - 1000 mV	Square	Down	N/A	60	1	0 mV	300-400 mV	600 - 1500	1/3 crystals
Crystalization	V	300 mV	Square	Up	60	30	3	600	300 mV	1200	4/4 crystals formed from one pipette
(-)	V	300 mV	N/A	N/A	N/A	N/A	N/A	N/A	N/A	N/A	No crystal
(+)	V	900 mV	N/A	N/A	N/A	N/A	N/A	N/A	N/A	N/A	Structure formed early on
Crystalization	i	110 nA	Saw Tooth	Down	3 - 20	Front: 1-19	3	0 nA	30 nA	600	No Crystals formed
Crystalization	i	30 nA	Saw Tooth	Up	20	Front: 19	3	110 nA	30 nA	600	No Crystals Formed

Table 3-1 Table of Pulse Induced Crystallization Experiments. This table shows experiments for optimizing pulse parameters to induce nucleation. It lists if there is a positive control (+), negative control (-), or if there is a crystallization experiment with pulse. It also will provide parameters for the pulses along with if a crystal formed. Some experiments have multiple attempts, which are be noted in the notes section.

Table 3.1 shows experiments that find a pulse waveform and conditions that induce nucleation. In the table, the type of experiment is listed, such as if it is a positive control, negative control, or a crystallization experiment with pulse. Also, this list provides the conditions in which the pulses were conducted. The positive control experiments are experiments that use a high current or voltage that have shown to be successful in inducing nucleation within a 30 minutes time period; however, using such a high bias created crystals with poor quality in terms of optically resolved shape. The negative control experiments are experiments that uses low potential or current that creates a bubble formation but does not nucleation within a 30 minutes experiment. The negative control needs to use the highest potential or current that does not nucleate consistently. An example of this would be if a system does not nucleate consistently at

300 mV, there is no need to go lower to 200 mV, and this will be used for the pulse experiments. Finally, there are the crystallization experiments with pulses. These experiments contain a single or multiple pulses with either a square waveform or a sawtooth waveform. Note the sawtooth is actually a modified triangular waveform. The table shows that the square waveform has induced nucleation; however, the triangular or sawtooth has never induced it.

There are limited experiments shown, and currently more pulse experiment are being performed; however, with the data already present, it appears that the square waveform should be focused on for pulse induced nucleation experiments. The data also suggests that pulses that start from a low bias and move to a higher bias and back down to a low bias, pulse up, are more successful than pulses that start at a high bias transition to a lower bias then move back up to a high bias, pulse up.

3.2 Precondition for black spot removal and more consistent starting conditions

It was noticed that before application of an applied bias the pipette tip would develop a spherical structure on the tip of the pipette. Due to this structures appearance it was named the "black spot" and will hereafter be refered to as such. Frequently, we noticed that formation of a structures at the end of the pipettes would occur at different times within our standard 1800 s experiments. We believed the black spot formation before applying a bias could be affecting the results of when the formation of a structure occurred. As the conditions around the tip of the pipette are thought to be critical to the early nucleation, a precondition procedure was developed to try and standardize the conditions before the application of bias. This involved removal of the black spot and an attempt to remove the streaming current often present prior to application of bias Experiments were performed by applying a negative bias to the system for some duration. The theory of this procedure is applying a negative bias, potential or current, should induce

migration of the positively charge protons from the hydrochloric acid and migrate insulin away from the pipette tip, which will inhibit and reverse the formation of the black spot at the end of the nanopipette tip. Figure 3.14 shows a current clamping experiment that demonstrates the reversal of the formation of a black spot formation.

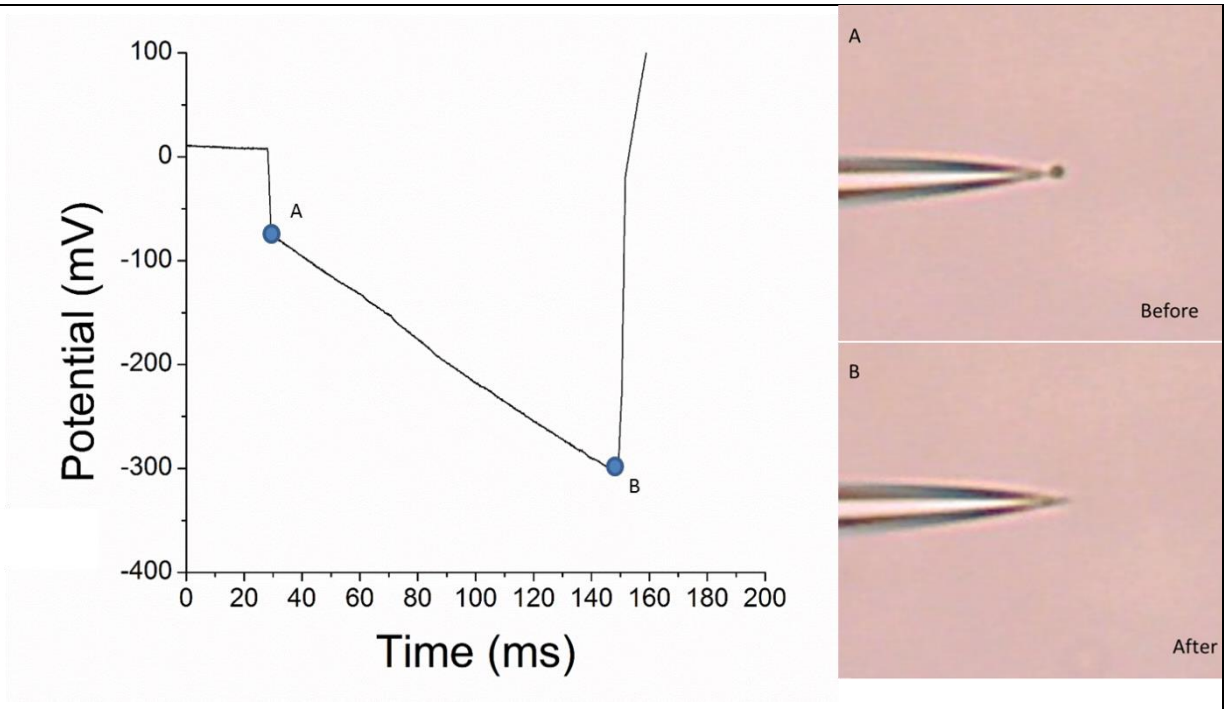

Figure 3-14 Application of Negative Bias Precondition for Black Spot Reversal. The main panel is the applied current graph for the current clamping experiment. Panel D is the voltage response curve of the current clamping experiment Image A is before applied bias of the current clamping experiment. Image B is during the end of the precondition step of the current clamping experiment..10x objective, 200nm pipette, 1M HCl, and 7.9 pH insulin solution.

In Figure 3.14 there is a demonstrated black spot reversal that was achieved by applying a negative bias. Image A shows a black spot structure on the end of the nanopipette that formed prior to the application of a bias. Formation of the black spot is likely due to diffusion of hydrochloric acid along the concentration gradient from the higher concentration inside the pipette to the lower concentration outside the tip of the pipette, inducing the formation. Image B

shows the black spot formation diminished on the nanotip. The image was taken near the end of the precondition step before the ramp stage. This is caused by the application of a negative bias. The main panel shows the programed applied current for the experiment with the application of -10nA for 120s. This application induced migration of the positively charged protons from the hydrochloric acid away from the nanopipette tip. This applied bias also causes migration of insulin protein away from the tip since in the pH 7.9 solution the insulin is negatively charged in solution. Which explains a reversal of the black spot formation at the tip. Here we can compare the optical results with the voltage response. As the negative potential is being applied to the system, the reversal of the black spot is optically shown. This suggests that the black spot formation is being reversed.

3.2.1 Optimizing Preconditions for More Consistent Starting Potentials

Preconditions were used to reverse the black spot formation that occurred when inserting the pipette into the solution and before a bias was applied. They were also used to make a system more consistent to influence transformation times to be more reproducible. After performing more experiments, it was noticed that performing consecutive experiments provided different starting responses. Here we are attempting to change the precondition parameters to eliminate the inconsistencies between multiple experiments. The experiments that used a constant bias, shown later, shows the inconsistencies between multiple experiments. The parameters for the experiments is shown in Figure 3.15

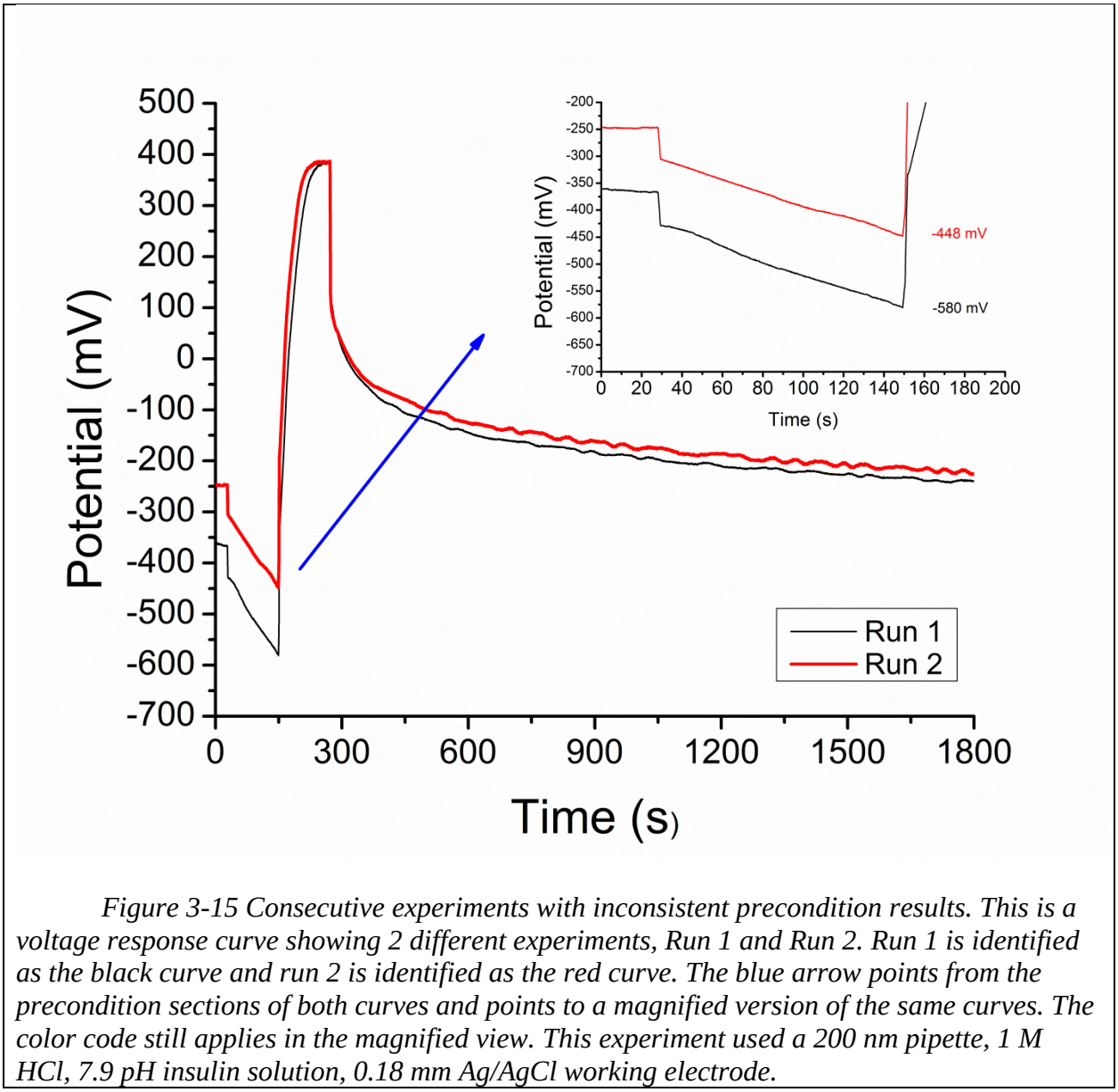

Figure 3-15 Consecutive experiments with inconsistent precondition results. This is a voltage response curve showing 2 different experiments, Run 1 and Run 2. Run 1 is identified as the black curve and run 2 is identified as the red curve. The blue arrow points from the precondition sections of both curves and points to a magnified version of the same curves. The color code still applies in the magnified view. This experiment used a 200 nm pipette, 1 M HCl, 7.9 pH insulin solution, 0.18 mm Ag/AgCl working electrode.

Figure 3.15 shows the voltage response curve with 2 different experiments. Both experiments use the same nanopipette and the same conditions. These experiments were taken in sequence. Different potential responses are obtained for both runs. In the magnified view, it can be observed that the first run's potential after precondition was -580 mV and the second run had a potential of -448 mV. There is a 132 mV difference between the first and second experiments. The starting potentials, time = 0, are -360 mV for the run 1 and -247 mV for run 2, which

provides a 113 mV difference. This deviation between runs is something that could directly affect consistency. This appears to be caused by using a constant current precondition.

The precondition does not have to be a constant current or potential, it can take on different waveforms e.g. sine, triangular, square. The duration and magnitude can also be changed as shown in Figure 3.16

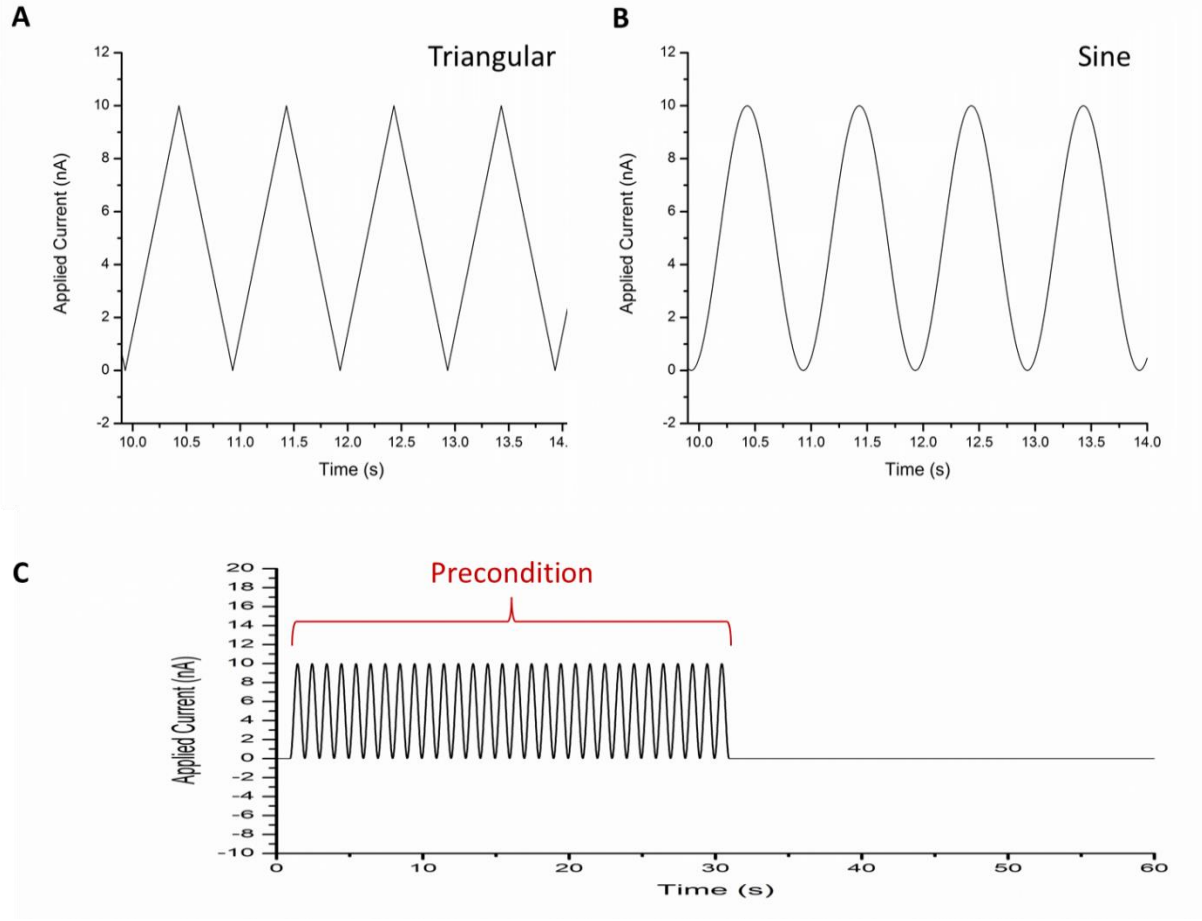

Figure 3-16 Different Alternate Precondition Waveforms. A) A graph displaying a section of the applied current conditions using a triangular waveform with a 10 nA bias and 1 Hz frequency. B) An applied current graph that uses a sine waveform with a 10 nA bias and 1 Hz frequency. C) A preconditioning experiment showing the applied current for a duration of 30 seconds applying 10 nA.

Figure 3.16 demonstrates some of the options other than a constant bias being applied to the system. A system can use a constant applied bias; however, it can also use an alternating

waveform such as a triangular or sine wave. We use different waveforms to test the effect on consistency and preventing black spot formation.

Fig. 3.16 A shows a triangular waveform being applied, using an amplitude of 10 nA at 1 Hz. Both the frequency and amplitude of the alternating current waveform can be adjusted.

Fig. 3.16 B displays a sine wave form that is applied to the system. This waveform applies a 10 nA peak bias and a 1 Hz frequency. The amplitude and the frequency can be changed along with duration of the the precondition.

Fig. 3.16 C illustrates an example of an experiment to test preconditions. This example applies a sine wave for 30 seconds. It applies 10 nA peak current at 1 Hz frequency. The duration for the experiment can be increased or decreased. Just like all of the waveforms shown in Figure 3.16 the amplitudes can be increased or decreased along with increasing or decreasing the frequency.

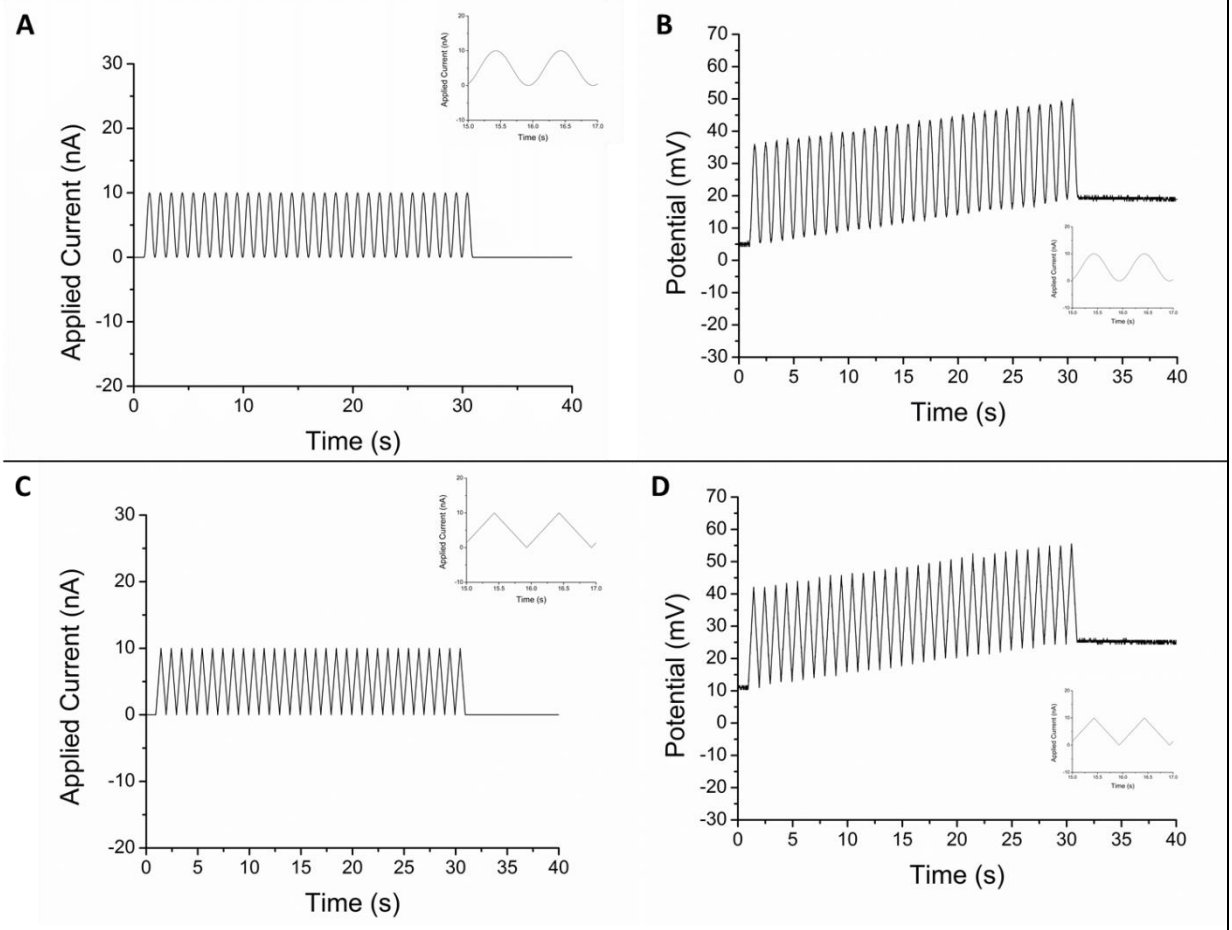

Figure 3-17 Using Alternating Current Preconditions to provide more reproducible starting potentials. The top half consists of a sine wave precondition. A) This is the applied current using a sine wave. B) This is the voltage response of the applied current that used a sine waveform. The bottom half consists of a triangular precondition. C) This is the applied current using a triangular wave. D) This is the voltage response of the applied current that used a triangular waveform.

Figure 3.18 displays four different curves that show the examples of two different alternating current waveforms, triangular and sine. The top half of the figure has two curves that represent the sine waveforms. There are insets added to each section displaying the waveform applied, for clearer viewing. The bottom half of the figure has two curves that represent the triangular waveform. These experiments use the same nanopipette and the same internal and external solution. The two experiments conducted were performed sequentially.

Fig 3.18 A is the applied current using a sine waveform at 10 nA held for 30 seconds at 1 Hz. The conditions frequency, amplitude, and duration can be adjusted.

Fig 3.18 B is the voltage response curve that was the made by Fig 3.18 A. It can be observed that there is a drift due to polarization from the positive bias being applied. The point of interest is where the alternating current application ends, indicated by the red dot. The other point used for analysis is the start of the experiment at t = 0. We can compare these points after running multiple experiments to see if by applying an alternating current waveform if we can achieve a more consistent preconditioning treatment before a ramp or maximum bias is applied.

Fig 3.18 C is the applied current using a triangular waveform which is held at 10 nA for 30 seconds at 1 Hz. Again these variables can be adjusted.

Fig 3.18 D is the voltage response curve that was the made by Fig 3.18 C. It can be observed that there is a drift due to polarization from the positive bias being applied. The point of interest is where the alternating current application ends, indicated by the red dot.

The observations made from conducting these experiments were that applying triangular waveforms were not as effective for reversing the black spot formation. We found that the triangular waveform would not provide a more consistent starting potential before applying the positive bias to the system for nucleation. Sine waveform was more successful for reversing and/or shrinking the black spot. The amplitudes tested were 500 mV and 100 mV in both the positive and negative polarities. Applying a negative bias greatly reduced black spot size to the scale where it was not visible. Applying a positive bias did not reverse the black spot. When testing the -100 mV and -500 mV a difference in reversing the black spot was not noticeable. The frequencies were also tested using a 10 Hz and a 1 Hz frequency. There was not a noticeable difference in reversing the black spot. While we found alternative ways to reverse the black spot

formation did not find a meaningful way to improve consistent starting potentials between consecutive experiments.

4 CONCLUSIONS

We have demonstrated active control of insulin nucleation using voltage and current clamping techniques with our device. We have taken it a step further by using square wave pulses to induce nucleation. The structure formed by the pulses does not appear to be ideal; however, with further optimization, it may be possible to nucleate with a controlled pulse and allow the crystal to grow using a constant current/potential bias. Triangular pulses have all shown not to trigger nucleation, but square wave pulses have shown great promise. More experiments need to be performed to optimize triggering nucleation.

Along with controlling crystal formation, we can observe the formations optically as they occur. Originally, we saw a black spot form at the nanopipette's tip, but with further testing and greater magnification, we believe we are viewing the dense liquid domain form. We noticed on this spherical structure a spot forming on the boundary where nucleation occurs, and crystals grow from this point. This supports theories that before nucleation occurs a dense liquid domain is created and somewhere within this domain, nucleation takes place. Theoretically, nucleation occurs within the dense liquid domain. We are currently testing this spherical structure to understand it better.

Other than using optical means for detecting nucleation, it has been demonstrated that during an optical change a conductive response occurs. Using both current and voltage clamping techniques, we have shown a signal response that occurs at the same moments as the structural change. The success rate for achieving a structural formation and a signal that coincides with the formation is about 30%.

In the future, these methods could be further developed to create a program that creates a black spot, uses a signal to trigger nucleation (like a pulse), and detect the signal response associated with nucleation to stop the pulse and switch to a bias that has shown the capabilities to grow a crystal with a lattice structure.

REFERENCES

1. Giegé, R., A historical perspective on protein crystallization from 1840 to the present day. *Febs J* **2013,** *280* (24), 6456-6497.
2. S. D. Durbin, G. F., Protein Crystallization *Phys Chem Chem Phys* **1996,** *47*, 171-204.
3. FERRY.*, R. M., STUDIES IN THE CHEMISTRY OF HEMOGLOBIN: I. THE PREPARATION STUDIES IN THE CHEMISTRY OF HEMOGLOBIN. *Journal of Biological Chemistry* **1923,** *57*, 819-828.
4. Derewenda, Z. S., Protein crystallization in drug design: towards a rational approach. *Expert Opin Drug Discov* **2007,** *2* (10), 1329-40.
5. Ragab, D.; Rohani, S.; Samaha, M. W.; El-Khawas, F. M.; El-Maradny, H. A., Crystallization of progesterone for pulmonary drug delivery. *J Pharm Sci* **2010,** *99* (3), 1123-37.
6. Desikan, S.; Anderson, S. R.; Meenan, P. A.; Toma, P. H., Crystallization challenges in drug development: scale-up from laboratory to pilot plant and beyond. *Curr Opin Drug Discov Devel* **2000,** *3* (6), 723-33.
7. Nanev, C. N., Recent experimental and theoretical studies on protein crystallization. *Cryst. Res. Technol.* **2016**, Ahead of Print.
8. Nanev, C. N.; Penkova, A.; Chayen, N., Effects of buoyancy-driven convection on nucleation and growth of protein crystals. *Ann N Y Acad Sci* **2004,** *1027*, 1-9.
9. Nanev, C. N.; Petrov, K. P., Steering a crystallization process to reduce crystal polydispersity; case study of insulin crystallization. *J. Cryst. Growth* **2016**, Ahead of Print.
10. Nanev, C. N.; Saridakis, E.; Chayen, N. E., Protein crystal nucleation in pores. *Sci Rep* **2017,** *7*, 35821.
11. Chen, D. L.; Gerdts, C. J.; Ismagilov, R. F., Using microfluidics to observe the effect of mixing on nucleation of protein crystals. *J Am Chem Soc* **2005,** *127* (27), 9672-3.
12. Chen, D. L.; Ismagilov, R. F., Microfluidic cartridges preloaded with nanoliter plugs of reagents: an alternative to 96-well plates for screening. *Curr Opin Chem Biol* **2006,** *10* (3), 226-31.
13. Hansen, C. L.; Skordalakes, E.; Berger, J. M.; Quake, S. R., A robust and scalable microfluidic metering method that allows protein crystal growth by free interface diffusion. *Proc Natl Acad Sci U S A* **2002,** *99* (26), 16531-6.
14. Hong, J.; Edel, J. B.; deMello, A. J., Micro- and nanofluidic systems for high-throughput biological screening. *Drug Discov Today* **2009,** *14* (3-4), 134-46.
15. Zheng, B.; Gerdts, C. J.; Ismagilov, R. F., Using nanoliter plugs in microfluidics to facilitate and understand protein crystallization. *Curr Opin Struct Biol* **2005,** *15* (5), 548-55.
16. Zhu, Y.; Zhu, L. N.; Guo, R.; Cui, H. J.; Ye, S.; Fang, Q., Nanoliter-scale protein crystallization and screening with a microfluidic droplet robot. *Sci Rep* **2014,** *4*, 5046.
17. Irene Russo Krauss , A. M., Alessandro Vergara and Filomena Sica An Overview of Biological Macromolecule Crystallization. *Int J Mol Sci* **2013,** *14* (6), 11643-11691.
18. Asherie, N., Protein crystallization and phase diagrams. *Methods* **2004,** *34* (3), 266-72.
19. Asherie, N., A dialogue about protein crystallization and phase diagrams. *Protein Pept Lett* **2012,** *19* (7), 708-13.
20. Haruhiko Koizumi, S. U., Kozo Fujiwara, Masaru Tachibana, Kenichi Kojima, and Jun Nozawa, Technique for High-Quality Protein Crystal Growth
by Control of Subgrain Formation under an External
Electric Field. *Multidisciplinary Digital Publishing Institute Crystals* **2016,** *6* (95).

21. Elizabeth Nieto-Mendozaa, B. A. F.-U., Gen Sazakib, Abel Moreno, Investigations on electromigration phenomena for protein crystallization using crystal growth cells with multiple electrodes: effect of the potential control. *Journal of Crystal Growth* **2005,** *275* (1-2), e1437–e1446.
22. Hou D, C. H., Ac Field enhanced protein crystallization. *Applied Physics Letter* **2008,** *92* (223902).
23. Ramachandran N, L. F., Using magnetic fields to control convection during protein crystallizationanalysis
and validation studies. *Journal of Crystal Growth* **2005,** *274* (297).
24. Christo N. Nanev*, V. D. T., and Feyzim V. Hodzhaoglu, Growth of Equally-Sized Insulin Crystals. Rostislaw Kaischew Institute of Physical Chemistry.
25. D. Hekmat, D. H., D. Weuster-Botz, *Chemical Engineering and Technology* **2008,** *31*, 911–916.
26. S. Pechenov, B. S., M.X. Yang, S.K. Basu, A.L. Margolin, Injectable controlled release formulations incorporating protein crystals. *Journal of Controlled*
Release **2003,** *16* (96(1)), 149-58.
27. S.K. Basu, C. P. G., C.W. Jung, A.L. Margolin, Expert opinion on biological therapy. *S.K. Basu, C.P. Govardhan, C.W. Jung, A.L. Margolin* **2004,** *4*, 301-317.
28. C. Govardhan, N. K., C.W. Jung, B. Simeone, A. Higbie, S. Qu, L. Chemmalil, S.; Pechenov, S. K. B., A.L. Margolin, *Pharm Res-Dordr* **2005,** *22*, 1461-1470.
29. Braatz, R. D., *Annual Reviews in Control* **2002,** *22*, 87–99.
30. F.F. Bonnichsen, P. N. J. 1999.
31. M. Jiang, M. H. W., Z. Zhu, J. Zhang, L. Zhou, K. Wang, A.N.F. Versypt, T. Si, L.M.; Hasenberg, Y.-E. L., R.D. Braatz,, *Chem Eng Sci* **2012,** *77*, 2-9.
32. Li, Y. Mass Transport Through Conical Nanopipettes and its Application in Energy Conversion and Crystallization. Dissertation, Georgia State University, 2015.
33. Kwon, J. H. K., C.W., *Journal of Crystal Growth* **2004,** *263* (1-4), 536-543.
34. Andrea Fortini∗ , E. S., and Marjolein Dijkstra, Crystallization and gelation in colloidal systems with short-ranged attractive
interactions. Debye Institute for NanoMaterials Science, Utrecht University: 2008.
35. Sujin Babu, J.-C. G., and Taco Nicola, Crystallization and dynamical arrest of attractive hard spheres. *THE JOURNAL OF CHEMICAL PHYSICS* **2009,** *130*.